

STRUCTURE OF ODD-ODD Ga AND As NUCLEI, DYNAMICAL AND SUPERSYMMETRIES

T.Fényes, A.Algora, Zs.Podolyák, D.Sohler, J.Timár

Institute of Nuclear Research of the Hungarian Academy of Sciences, 4001 Debrecen, Hungary

S.Brant, V.Paar, Lj.Šimičić

Department of Physics, Faculty of Science, University of Zagreb, 41000 Zagreb, Croatia

The structure of ^{66}Ga , ^{68}Ga , ^{70}Ga , ^{70}As , ^{72}As , ^{73}As , ^{74}As , and ^{76}As was studied via $(p, n\gamma)$ (and in some cases) $(\alpha, n\gamma)$ reactions. In-beam γ -ray, two-dimensional $\gamma\gamma$ -coincidence, internal conversion electron, and γ -ray angular distribution spectra, as well as $\sigma(E_{\text{LEV}}, E_p)$ relative reaction cross sections were measured with Ge(HP), Ge(Li) γ and combined superconducting magnetic plus Si(Li) electron spectrometers at different bombarding particle energies. The proposed new level schemes contain 300 (among them 70 new) levels. Level spins, parities, γ -ray branching and mixing ratios have been deduced. Energy spectra, electromagnetic moments, reduced transition probabilities, γ -ray branching ratios, and one-nucleon transfer reaction spectroscopic factors were calculated in the framework of interacting boson model (IBM), interacting boson-fermion model (IBFM), and interacting boson-fermion-fermion model (IBFFM) for about 20 nuclei in the Ga-As region ($^{64-67}\text{Zn}$, $^{65-68}\text{Ga}$, $^{68-73}\text{Ge}$, $^{70-74}\text{As}$). The odd-odd nuclei were described on the basis of consistent parametrization deduced from the even-even core and the two neighbouring odd-A nuclei. Reasonable description of experimental data has been obtained. The energy splitting of proton-neutron multiplets in odd-odd Ga and As nuclei is discussed also with the use of the parabolic rule which is associated with IBFFM in the low perturbation order. The energy spectra of $^{74}\text{Se}_{40}$, $^{75}\text{Se}_{41}$, $^{73}\text{As}_{40}$, $^{74}\text{As}_{41}$ supermultiplet nuclei were calculated on the basis of the $U_{\pi}(6/12) \otimes U_{\nu}(6/12)$ supersymmetry (SUSY) theory, using a simple closed energy formula. 44 states of these four different nuclei have been reasonably described using only 7 fitted parameters. The existence of supersymmetry was supported also by one-nucleon transfer reaction data, electromagnetic properties, as well as by IBFM, IBFFM and SUSY model wave functions of the levels considered.

Изучена структура ядер ^{66}Ga , ^{68}Ga , ^{70}Ga , ^{70}As , ^{72}As , ^{73}As , ^{74}As и ^{76}As через реакции $(p, n\gamma)$ и (в некоторых случаях) $(\alpha, n\gamma)$. Измерены спектры γ -лучей, двумерных $\gamma\gamma$ -совпадений, электронов внутренней конверсии и углового распределения γ -лучей, а также $\sigma(E_{\text{ур}}, E_p)$ относительные поперечные сечения реакций с помощью Ge(HP),

Ge(Li) γ -детекторов и сверхпроводящего магнитного Si(Li)-спектрометра электронов при различных энергиях бомбардирующих частиц. Предложенные новые схемы уровней содержат 300 (между ними 70 новых) уровней. Приведены спины, четности, коэффициенты γ -разветвления и смешивания. Рассчитаны энергетические спектры, электромагнитные моменты, приведенные вероятности переходов, коэффициенты γ -разветвления и спектроскопические факторы в рамках модели взаимодействующих бозонов (фермионов) (МБФ (Ф)) для ≈ 20 ядер в области Ga-As ($^{64-67}\text{Zn}$, $^{65-68}\text{Ga}$, $^{68-73}\text{Ge}$, $^{70-74}\text{As}$). Нечетно-нечетные ядра описываются параметрами, полученными из приспособления к экспериментальным данным о свойствах ядра четно-четного остова и двух соседних ядер с нечетными массовыми числами. Получено разумное описание экспериментальных данных. Энергетическое расщепление протон-нейтрон мультиплетов в нечетно-нечетных ядрах Ga и As обсуждается с помощью параболического правила, ассоциированного с МБФ в низком порядке возмущения. Рассчитаны энергетические спектры супермультиплета ^{74}Se , ^{75}Se , ^{73}As и ^{74}As на базе теории $U_{\pi}(6/12) \otimes U_{\nu}(6/12)$ суперсимметрии (СУСИ). Описаны расчеты 44 уровней четырех различных ядер с использованием только семи подгоночных параметров. Существование суперсимметрии подтверждено данными реакций однонуклонных передач, электромагнитными свойствами, а также МБФ и СУСИ волновыми функциями обсуждаемых уровней.

1. INTRODUCTION

The main intention of the present work was a detailed in-beam γ - and electron-spectroscopic study of the odd-odd Ga and As isotopes and a consistent description of the structure of the Zn, Ga, Ge, and As nuclei in the framework of the interacting boson (-fermion-fermion) model (IB(FF)M). The nuclei, investigated in this program, are shown in Fig.1.

The experimental work was motivated by the fact, that the level systems of the investigated odd-odd nuclei (and especially the level spin and parity values) were known very scantily. For example, in ^{68}Ga unambiguous spin-parity data had been determined only for three levels before our measurements. The beams of the Debrecen isochronous cyclotron enabled excitation both of particle and collective states, and the high resolution, high efficiency Ge(HP) detectors and unique superconducting magnetic electron spectrometer, constructed in the Institute of Nuclear Research, assured good possibility for complex γ - and electron-spectroscopic in-beam studies.

A theoretical interpretation of the ^{66}Ga and ^{68}Ga level schemes was formerly completely missing. In the case of $^{70,72,74}\text{As}$ we have performed interacting boson-fermion-fermion model calculations for the first time. These calculations gave consistent and detailed description of the energy spectra and electromagnetic properties of the corresponding even-even, odd-A and odd-odd Zn, Ga, Ge, and As nuclei.

Z										
34 Se							<u>74</u>	<u>75</u>		
33 As			69	<u>70</u>	71	<u>72</u>	<u>73</u>	<u>74</u>	<u>75</u>	<u>76</u>
32 Ge			68	69	70	71	72	73	74	75
31 Ga	65	<u>66</u>	67	<u>68</u>	69	<u>70</u>				
30 Zn	64	65	66	67	68	69				
	34	35	36	37	38	39	40	41	42	43 N

Fig.1. Nuclei, investigated in this program experimentally, are indicated by eight mass numbers in solid frames. Mass numbers in dotted frames: theoretical calculations; Z: atomic, N: neutron numbers; mass number underlined with a thick line: stable nucleus

The new experimental data, obtained on ^{73}As and ^{74}As , offered possibility of checking the supersymmetry predictions for ^{74}Se , ^{75}Se , ^{73}As , and ^{74}As nuclei.

2. EXPERIMENTAL METHODS AND RESULTS

We have studied the excited states of the Ga and As nuclei in the proton and α -particle beams of the Debrecen 103-cm (and in some experiments of the Jyväskylä 90-cm) isochronous cyclotrons via $(p, n\gamma)$ and $(\alpha, n\gamma)$ reactions. The targets were prepared from enriched Cu, Zn, and Ge isotopes. The description of the spectroscopic channels of the Debrecen cyclotron can be found in Refs. [1,2].

High-resolution Ge (HP and LEPS) detectors were used for γ - and a superconducting magnetic lens plus Si(Li) spectrometer (SMLS) for electron-spectroscopic measurements. The SML spectrometer, which was described in detail in [3], has high transmission, good energy resolution, and low background.

In order to obtain «complete» spectroscopic information, γ -ray (E_γ, I_γ), $\gamma\gamma$ -coincidence, internal conversion electron and γ -ray angular distribution spectra, as well as relative reaction cross section $\sigma_{\text{rel}}(E_{\text{LEV}}, E_p)$ were measured

at different bombarding particle energies. Level schemes, spin-parity values, γ -branching and γ -mixing ratios have been deduced. Great attention was paid to the reliability and consistency of the obtained data. For example, the level spins have been determined with three different methods: a) from the decay properties and internal conversion coefficients of transitions, b) from Hauser-Feshbach analysis of the (p, n) reaction cross sections, and c) from γ -ray angular distributions. Configuration of levels has been determined from all available data: from nucleon transfer reaction studies, log ft values of β -decay, electromagnetic moments, transition probabilities, γ -branching ratios, predictions of parabolic rule calculations, etc.

As a result of experimental work about 880 (among them 440 new) γ rays have been identified, 280 (including 240 new) α_K internal conversion coefficients and ~ 300 (among them 70 new) levels have been determined in $^{66,68,70}\text{Ga}$ and $^{70,72,73,74,76}\text{As}$ nuclei.

The results have been published in the following papers: ^{66}Ga [4,13], ^{68}Ga [5,6,13], ^{70}Ga [7], ^{70}As [8], ^{72}As [9,13], ^{73}As [10], ^{74}As [11—13], and ^{76}As [14]. These works contain detailed description of the experimental methods and results, deduced new level schemes, and their discussion. The level spectra were based mainly on $\gamma\gamma$ -coincidence relations, as well as on energy and intensity balance of transitions.

3. SYSTEMATICS OF THE EVEN-EVEN AND SINGLE-ODD NUCLEI IN THE Zn-Se REGION

If we want to describe the structure of odd-odd nuclei, we need to know the energy levels of the neighbouring even-even and odd-A nuclei. The systematics of the 0_1^+ , 2_1^+ , 4_1^+ , and 3_1^- states of the even-even Zn, Ge, and Se nuclei is shown in Fig.2. The low-lying levels of the odd-A Zn, Ga and Ge, As nuclei are presented in Figs.3 and 4, respectively. The main configurations of states are also indicated in Figs.3 and 4 on the basis of one-nucleon transfer reaction and other available data.

The systematics of neutron quasiparticle energies and occupation probabilities in the Ni-Se region are shown in Fig.5.

In order to get preliminary estimates for the configurations of the low-lying levels of odd-odd Ga and As nuclei, we have performed parabolic rule [16] calculations. These calculations proved very useful for the prediction of the energy splitting of different proton-neutron multiplets in odd-odd In [1] and Sb [2] nuclei. In the Ga and As isotopes rather strong configuration mixing is expected among the close-lying identical spin-parity states, which may imply limitation on the applicability of the parabolic rule. Nevertheless, it can be used for the first orientation, as indeed the IBFFM calculations showed later.

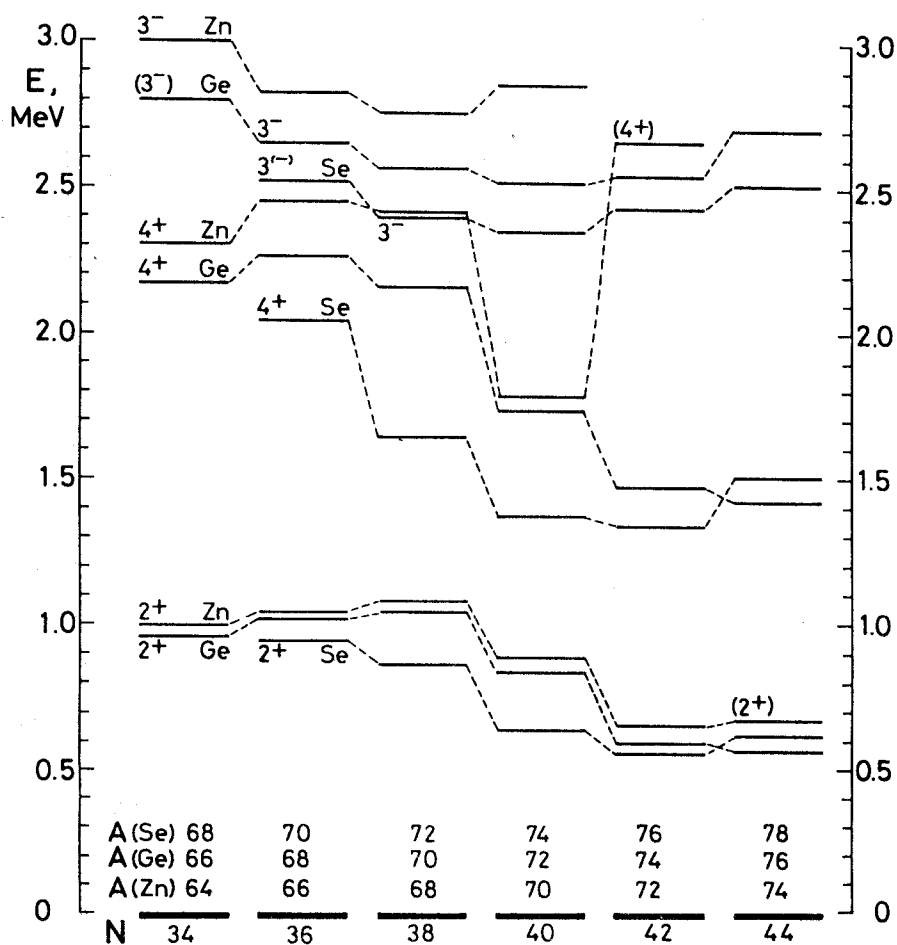


Fig.2. Energies of 2_1^+ , 4_1^+ and 3_1^- states of the even-even Zn, Ge and Se nuclei. Data were taken from the corresponding Nuclear Data Sheets

As the parabolic rule and its applications to In and Sb nuclei were described in detail in [16, 1 and 2], here we show only the results obtained on the relative energy splitting of proton-neutron multiplets in ^{70}As (Fig.6) and $^{66,68,70}\text{Ga}$, $^{70,72,74,76}\text{As}$ nuclei (Fig.7). In these predictions the same proton and neutron occupation probabilities were used, as later in the IBFFM calculations (see Section 4).

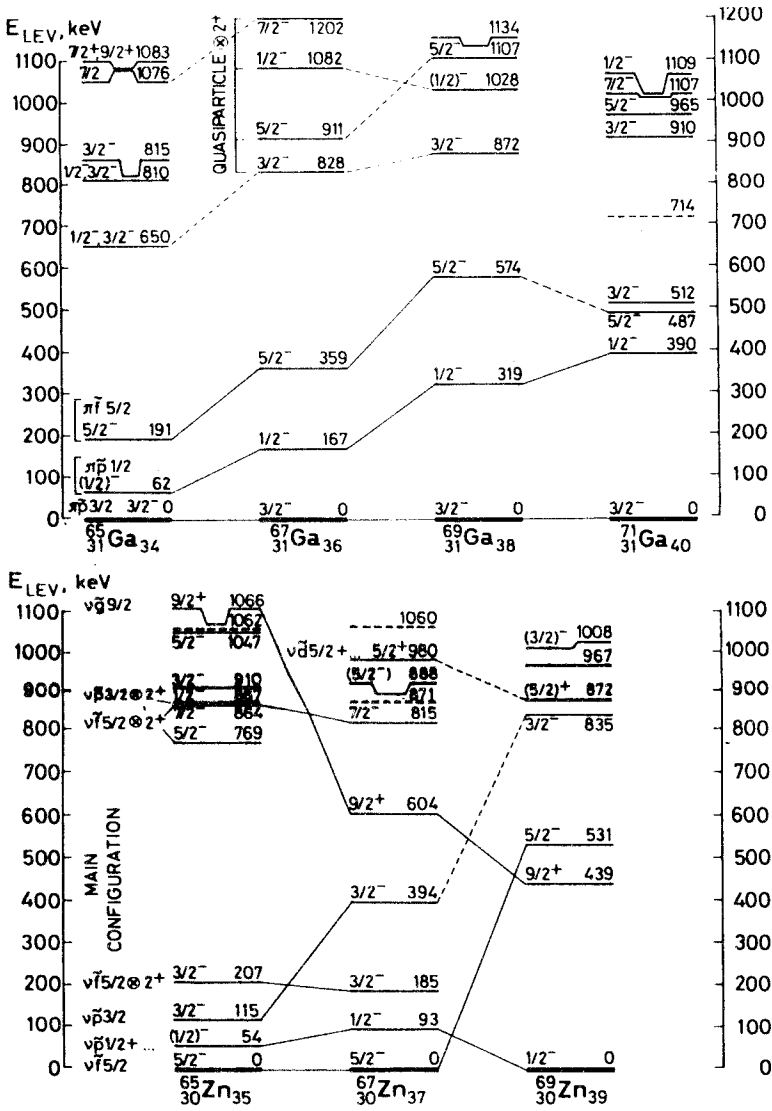


Fig.3. The low-lying levels of odd-A $^{65-69}\text{Zn}$ and $^{65-71}\text{Ga}$ nuclei. Data were taken from the corresponding Nuclear Data Sheets and original papers

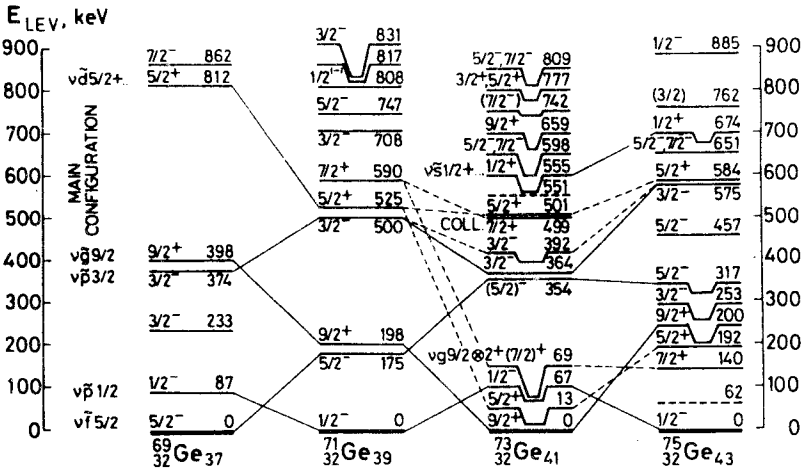
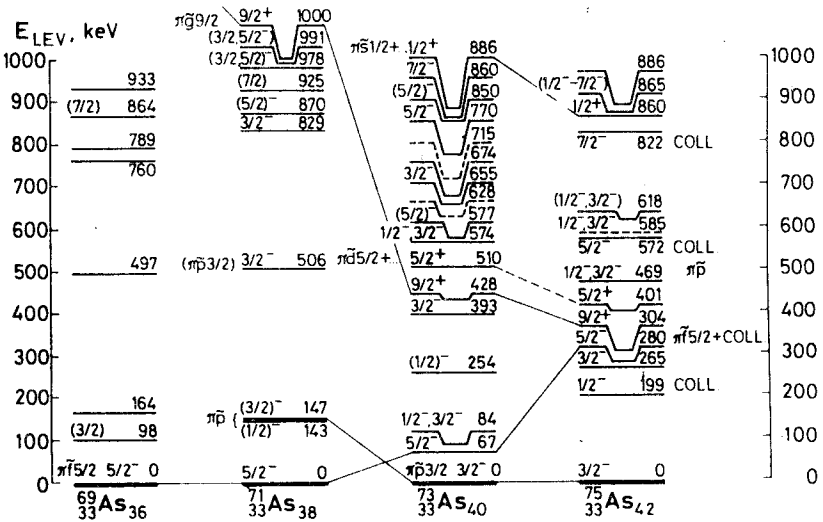


Fig.4. The low-lying levels of odd-A $^{69-75}\text{Ge}$ and $^{69-75}\text{As}$ nuclei. Data were taken from the corresponding Nuclear Data Sheets and original papers

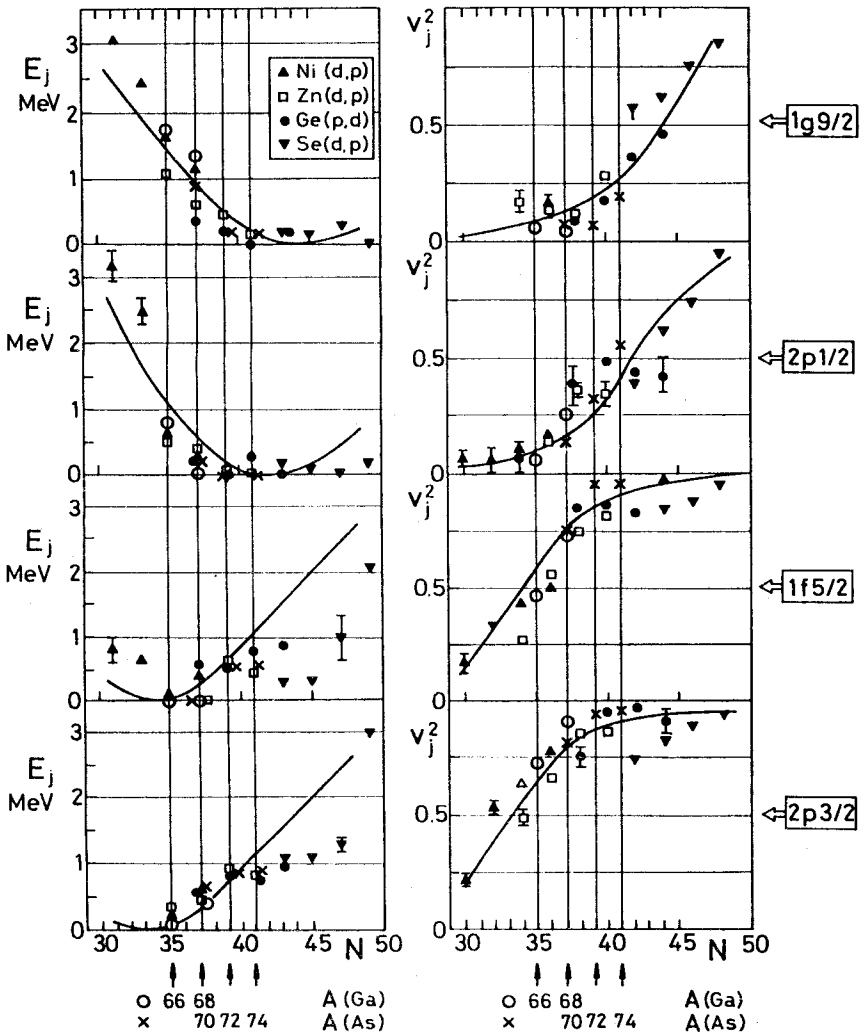


Fig.5. Experimental quasi-particle energies (E_j) and occupation probabilities as a function of the neutron number (N) (points) and the corresponding BCS theoretical results (curves). Data were taken from Fournier et al. [15]. Values used in the present calculations are shown by circles (o) for Ga and crosses (x) for As odd-odd nuclei

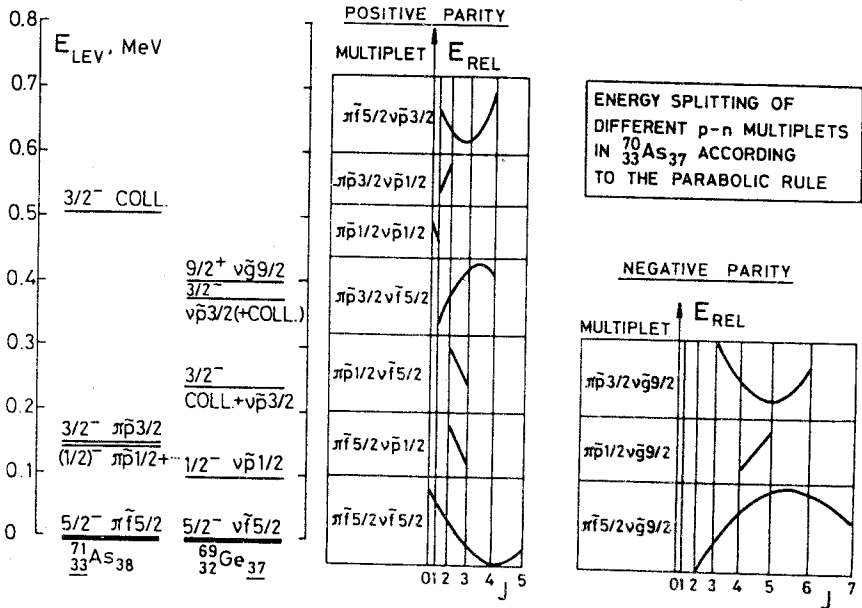


Fig.6. Approximate relative energy splitting of different $p-n$ multiplets in ^{70}As , as predicted by the parabolic rule. The abscissa is scaled according to $J(J+1)$, where J is the spin of the state

4. INTERACTING BOSON-(FERMION-FERMION) MODEL CALCULATIONS

In order to get deeper and more detailed insight into the structure of the low-lying odd-odd Ga and As states, we have calculated the level energies and electromagnetic properties on the basis of the interacting boson-(fermion-fermion) model.

4.1. Hamilton operator. The Hamiltonian of the model is [17—20]:

$$H_{\text{IBFFM}} = H_{\text{IBFM}}(\pi) + H_{\text{IBFM}}(\nu) - H_{\text{IBM}} + H_{\text{RES}}(\pi\nu), \quad (1)$$

where H_{IBM} denotes the IBM Hamiltonian for the even-even core nucleus [21—22], $H_{\text{IBFM}}(\pi)$ and $H_{\text{IBFM}}(\nu)$ are the IBFM Hamiltonians for the neighbouring odd-even nuclei with an odd proton and odd neutron, respectively [23—25], and $H_{\text{RES}}(\pi\nu)$ is the Hamiltonian of the residual interaction.

The Hamiltonian of the core has the following form [26—28]

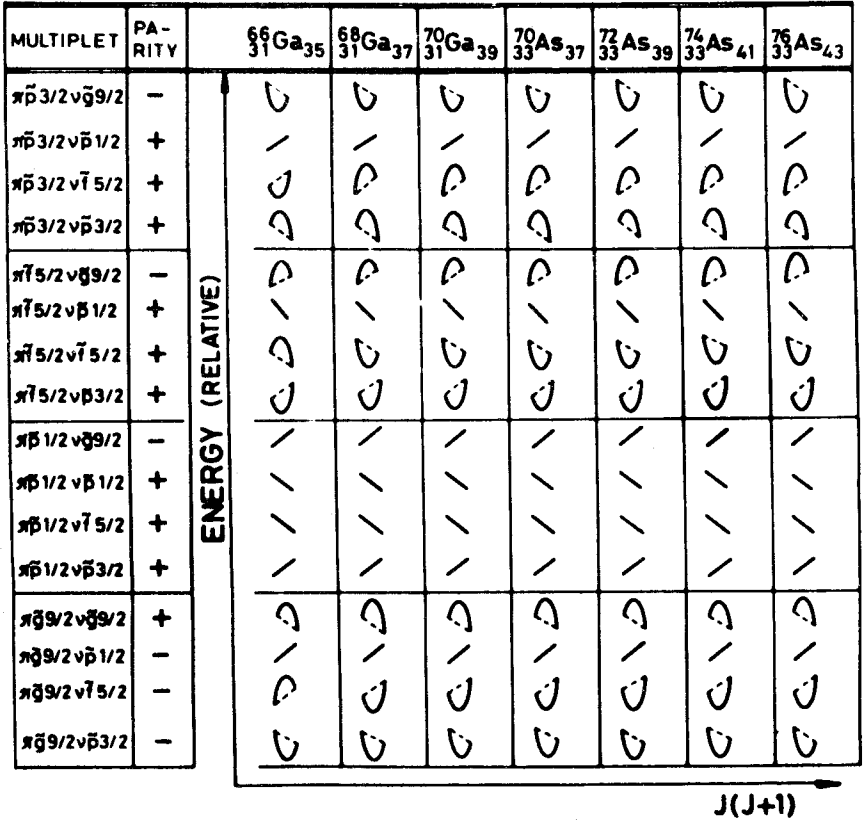


Fig.7. Approximate relative energy splitting of different proton-neutron multiplets in some odd-odd Ga and As nuclei as a function of $J(J + 1)$. J is the spin of the state. The predictions were based on the parabolic rule

$$\begin{aligned}
 H_{IBM} = & h_1 \hat{N} + h_2 \{ (d^+ d^+)_0 [(N - \hat{N})(N - \hat{N} - 1)]^{1/2} + h.c. \} + \\
 & + h_3 \{ (d^+ d^+ \tilde{d})_0 (N - \hat{N})^{1/2} + h.c. \} + \sum_{L=0,2,4} h_{4L} [(d^+ d^+)_L (\tilde{d}\tilde{d})_L]_0, \quad (2)
 \end{aligned}$$

where \hat{N} is the d -boson number operator and N is the total number of s and d bosons. The relation of $\{h\}$ parameters to the parameters defined in Ref.[21] is as follows:

$$h_1 = \epsilon_d - \epsilon_s + \left(\frac{1}{\sqrt{5}} u_2 - u_0 \right) (N - 1),$$

$$h_2 = \frac{1}{\sqrt{2}} \tilde{v}_0, \quad h_3 = \tilde{v}_2, \quad (3)$$

$$h_{4L} = \sqrt{2L+1} \left(\frac{1}{2} c_L - \frac{1}{\sqrt{5}} u_2 + \frac{1}{2} u_0 \right).$$

The IBFM Hamiltonian employed here is of the form [27]

$$H_{\text{IBFM}}(\alpha) = H_{\text{IBM}} + \sum_i \tilde{\epsilon}_i(\alpha) + H_{\text{BF}}(\alpha), \quad (4)$$

where α stands for odd proton ($\alpha = \pi$) or neutron ($\alpha = \nu$). The second and third terms are the quasiparticle and boson-fermion (particle-vibration) interaction Hamiltonians, respectively.

$$\begin{aligned} H_{\text{BF}}(\alpha) = & \sum_j A_j \{ (d^+ \tilde{d})_0 [c_j^+(\alpha) \tilde{c}_j(\alpha)]_0 \}_0 + \\ & + \sum_{j_1 j_2} \Gamma_{j_1 j_2} \{ Q_2 [c_{j_1}^+(\alpha) \tilde{c}_{j_2}(\alpha)]_2 \}_0 + \\ & + \sum_{j_1 j_2 j_3} \Lambda_{j_1 j_2 j_3} : \{ [c_{j_1}^+(\alpha) \tilde{d}]_{j_3} [\tilde{c}_{j_2}(\alpha) d^+]_{j_3} \}_0 : , \end{aligned} \quad (5)$$

with

$$A_j = A_0 \sqrt{5} (2j+1), \quad (6)$$

$$\Gamma_{j_1 j_2} = \Gamma_0 \sqrt{5} (u_{j_1} u_{j_2} - v_{j_1} v_{j_2}) \langle j_1 \| Y_2 \| j_2 \rangle, \quad (7)$$

$$\begin{aligned} \Lambda_{j_1 j_2 j_3} = & -2\Lambda_0 \frac{\sqrt{5}}{\sqrt{2j_3+1}} (u_{j_1} v_{j_3} + v_{j_1} u_{j_3}) (u_{j_3} v_{j_2} + v_{j_3} u_{j_2}) \times \\ & \times \langle j_3 \| Y_2 \| j_1 \rangle \langle j_3 \| Y_2 \| j_2 \rangle, \end{aligned} \quad (8)$$

$$Q_{2\mu} = d_\mu^+ \sqrt{N - \hat{N}} + \sqrt{N - \hat{N}} \tilde{d}_\mu + \chi (d^+ \tilde{d})_{2\mu}. \quad (9)$$

The Hamiltonian of the residual interaction was taken in the form

$$\begin{aligned} H_{\text{RES}}(\pi\nu) = & 4\pi V_\delta \delta(\mathbf{r}_\pi - \mathbf{r}_\nu) \delta(r_\pi - R_0) - \sqrt{3} V_{\sigma\sigma} (\boldsymbol{\sigma}_\pi \cdot \boldsymbol{\sigma}_\nu) + \\ & + V_{\text{tens}} \left[\frac{3(\boldsymbol{\sigma}_\pi \cdot \mathbf{r}_{\pi\nu})(\boldsymbol{\sigma}_\nu \cdot \mathbf{r}_{\pi\nu})}{r_{\pi\nu}^2} - (\boldsymbol{\sigma}_\pi \cdot \boldsymbol{\sigma}_\nu) \right], \end{aligned} \quad (10)$$

where $\mathbf{r}_{\pi\nu} = \mathbf{r}_\pi - \mathbf{r}_\nu$, $R_0 = 1.2 \sqrt{A}$ fm. $H_{\text{RES}}(\pi\nu)$ includes surface delta, spin-spin and tensor interactions.

Hamiltonian (1) was diagonalized in the proton-neutron-boson basis: $|(j_\pi, j_\nu) j_{\pi\nu}, n_d^I; J\rangle$, where j_π and j_ν stand for the proton and neutron angular

moments coupled to $j_{\pi\nu}$, n_d is the number of d bosons, l is their angular momentum, and J is the spin of the state. The computer codes, used in the calculations, were written by Brant, Paar and Vretenar [29].

4.2. Method of calculation. Parametrization. In the first step of calculations we have fitted the $\{h_i\}$ parameters of the H_{IBM} Hamiltonian (2) to the energy spectrum of the corresponding core nuclei (^{64}Zn , ^{66}Zn , ^{68}Ge , ^{70}Ge , and ^{72}Ge).

The total boson number is given by the number of valence shell pairs. For example, in $^{66}\text{Zn}_{36}$ (the core of $^{68}_{31}\text{Ga}_{37}$) $N=5$, since in this nucleus there are one proton plus four neutron bosons, relative to the $Z=N=28$ double magic nucleus. In the case of $^{70}\text{Ge}_{38}$ (the core of $^{72}_{33}\text{As}_{39}$) and $^{71}\text{Ge}_{39}$ the calculations were performed both with $N=7$ and $N=4$. Both calculations, with renormalization of the other parameters, gave similar results for the energy spectra and electromagnetic properties [9]. Thus in the further calculations for ^{70}As , ^{72}As , ^{74}As , and neighbouring 9 nuclei we have used reduced total boson numbers, by renormalizing the IBM parameters. This strongly reduced the scope of computations for odd-odd nuclei, without a substantial effect on the properties of the low-lying states.

The χ and vibrational charge (e^{VIB}) parameters were fitted to the electromagnetic moments and reduced B(E2) transition probabilities of the core nuclei.

^{66}Zn exhibits level scheme, which is characteristic of a spherical vibrator. In this case the h_2 and h_3 parameters were chosen to be equal to zero. In other nuclei we have employed parametrization, which corresponds to a transition between the U(5) and SU(3) dynamical symmetries, but somewhat closer to the U(5) character.

The core parameters, employed in the calculations, are given in the first part of Table 1.

In the second step of calculations we have adjusted the parameters of $H_{\text{IBFM}}(\pi)$ (4—8) to the experimental data of the corresponding odd- Z , even- N nuclei. The proton quasiparticle energies and occupation probabilities were taken mostly from proton transfer reaction data and/or pairing force (BCS) calculations.

The A_0^π monopole, Γ_0^π dynamical quadrupole, and Λ_0^π exchange boson-fermion interaction strengths were fitted to the low energy spectra of ^{65}Ga , ^{67}Ga , ^{71}As , and ^{73}As , respectively. (The level spectrum of ^{69}As was very scarcely known). The g_s^π and g_{tens}^π effective gyromagnetic ratios have been determined from the fitting to the electromagnetic moments and reduced B(E2), B(M1) transition probabilities (γ -branching ratios).

Table 1. Parameters of the IBFFM calculations

Parameters		$^{66}_{31}\text{Ga}_{35}$	$^{68}_{31}\text{Ga}_{37}$	$^{70}_{33}\text{As}_{37}$	$^{72}_{33}\text{As}_{39}$	$^{74}_{33}\text{As}_{41}$
Core, MeV	h_1	0.8	1.039	0.9	0.88	0.68
	h_2	-0.2	0	-0.15	-0.3	-0.25
	h_3	0	0	0.06	0.12	0.1
	h_{40}	0.1	0.147	0	0.2	0
	h_{42}	-0.15	-0.2292	-0.5	-0.4	-0.3
	h_{44}	0.3	0.5595	-0.08	-0.08	-0.08
Total boson N^0 ,	N	4	5	3	4 (or 7)	4
	χ	-0.5	-0.5	-1.323*	-1.323*	-1.323*
e	e^{VIB}	1.35	1.35	0.8	0.8	0.8
Quasi-proton energy, MeV	$E(\pi p 3/2)$	0	0	0.3	0	0
	$E(\pi f 5/2)$	0.75	0.75	0	0.41	0.41
	$E(\pi p 1/2)$	0.615	0.615	0.3	0.74	0.74
	$E(\pi g 9/2)$			1.3	2.2	1.55
	$E(\pi d 5/2)$				5.2	4.55
Occup. probability	$V^2(\pi p 3/2)$	0.6	0.6	0.607	0.607	0.579
	$V^2(\pi f 5/2)$	0.07	0.07	0.309	0.309	0.341
	$V^2(\pi p 1/2)$	0.09	0.09	0.131	0.131	0.118
	$V^2(\pi g 9/2)$			0.07	0.07	0.06
	$V^2(\pi d 5/2)$				0.01	0.01
Quasi-neutron energy, MeV	$E(\nu p 3/2)$	0.09	0.49	0.60	0.95	0.95
	$E(\nu f 5/2)$	0	0	0	0.53	0.53
	$E(\nu p 1/2)$	0.83	0.03	0.2	0	0
	$E(\nu g 9/2)$	1.69	1.36	0.9	0.2	0.2
	$E(\nu d 5/2)$				3.2	3.2
Occup. probability	$V^2(\nu p 3/2)$	0.73	0.89	0.80	0.941	0.957
	$V^2(\nu f 5/2)$	0.48	0.73	0.75	0.949	0.962
	$V^2(\nu p 1/2)$	0.11	0.25	0.16	0.327	0.624
	$V^2(\nu g 9/2)$	0.08	0.04	0.09	0.09	0.217
	$V^2(\nu d 5/2)$				0.01	0.01
Strengths of boson-fermion interaction, MeV	A_0^π	0.05	0.05	0.05	0.05	0.05
	Γ_0^π	0.48	0.4	0.4	0.5	0.5
	Λ_0^π	1.4	0.5	0.5	0.5 π +	0.5
				1.5 π -		

Parameters		$^{66}_{31}\text{Ga}_{35}$	$^{68}_{31}\text{Ga}_{37}$	$^{70}_{33}\text{As}_{37}$	$^{72}_{33}\text{As}_{39}$	$^{74}_{33}\text{As}_{41}$
	A_0^v	0	0	0	0	0
	Γ_0^v	0.02	0.15	0.2	$0.55\pi +$ $0.45\pi -$	0.55
	Λ_0^v	1.63	1.3	1.3	$1.30\pi +$ $5.50\pi -$	$1.3\pi +$ $5.5\pi -$
Effective gyromagn. ratios	g_s^π	$0.4g_s^{\pi,f} \square$	$0.4g_s^{\pi,f}$	$0.40g_s^{\pi,f} \pi +$ $0.65g_s^{\pi,f} \pi -$	$0.7g_s^{\pi,f}$	$0.7g_s^{\pi,f}$
	$g_{\text{tens}}^{\pi **}$	1.56	$1.59 \diamond$	0	3.340	3.372
	g_s^v	$0.9g_s^{v,f} \nabla$	$0.5g_s^{v,f} \pi +$ $0.9g_s^{v,f} \pi -$	$0.4g_s^{v,f}$	$0.7g_s^{v,f}$	$0.7g_s^{v,f}$
	$g_{\text{tens}}^{v **}$	-1.07	-1.09Δ	0	-4.40	-4.48
Strengths of residual interaction, MeV	V_δ	-0.4	-0.4	$0 \pi +$ $-0.4 \pi -$	$0 \pi +$ $-0.6 \pi -$	$0 \pi +$ $-0.6 \pi -$
	$V_{\sigma\sigma}$	0.4	0.4	$0.4 \pi +$ $0.3 \pi -$	0	0
	V_{tens}	-0.01	0.015	0.015	0.015	0.015

$e^\pi = 1.5e$, $e^v = 0.5e$, $g_l^\pi = 1$, $g_l^v = 0$, $g_R = Z/A$ in all cases

$$* 1.323 = \sqrt{7/2}$$

$\pi +$ and $\pi -$ stand for positive and negative parity states, respectively

**The tensor gyromagnetic ratio, $g_{\text{tens}}^{\pi,v}$ [59,60] is similar to the one used in ref.[61]

$$\diamond \frac{1}{50} \langle r^2 \rangle g_s^\pi (\text{free}) = 1.59; \Delta \frac{1}{50} \langle r^2 \rangle g_s^v (\text{free}) = -1.09$$

$$\square g_s^{\pi,f} = g_s^\pi (\text{free}) = 5.5857$$

$$\nabla g_s^{v,f} = g_s^v (\text{free}) = -3.8263$$

In the third step of calculations we adjusted the A_0^v , Γ_0^v , and Λ_0^v parameters of $H_{\text{IBFM}}(v)$ (4—8) to the low-energy spectra of the corresponding even-Z, odd-N nuclei: ^{65}Zn , ^{67}Zn , ^{69}Ge , ^{71}Ge , and ^{73}Ge . The proton quasiparticle energies and occupation probabilities were close to the calculated BCS values of Ref.[15], and to the systematics of experimental data (Fig.5). The g_s^v and g_{tens}^v parameters were fitted to the electromagnetic properties.

Finally the V_δ , $V_{\sigma\sigma}$ and V_{tens} parameters of the residual interaction (10) were fitted to the experimental data of odd-odd nuclei. The core parameters and

occupation probabilities remained unaltered in all cases. We remark that in ^{70}As , ^{72}As , and ^{74}As readjustment of quasiparticle energies, boson-fermion interaction strengths and effective gyromagnetic ratios was needed in order to have better agreement with the experimental data. Such a renormalization seems to be in accordance with general observation in the regions of soft nuclei: the dynamical deformation can be sizeable, if one nucleon is added. Consequently, the parameters may change sizeably from those derived from the neighbouring nuclides. Similar feature was found, for example, in the $A = 130$ region.

The parameters applied for the IBFFM description of the properties of the odd-odd nuclei are summarized in Table 1.

4.3. Results. Discussion. The calculated energy spectra are compared with the experimental data in Figs.8 (^{64}Zn , ^{65}Ga), 9(^{65}Zn , ^{66}Ga), 10(^{66}Zn , ^{67}Ga), 11(^{67}Zn , ^{68}Ga), 12(^{68}Ge , ^{69}Ge , ^{70}As), 13(^{70}Ge , ^{71}As), 14(^{71}Ge , ^{72}As), 15(^{72}Ge , ^{73}As), and 16(^{73}Ge , ^{74}As). Although the level schemes are usually very complicated (especially in odd-odd nuclei), reasonable agreement has been obtained between experiment and theory. The calculated states are assigned to the experimental levels usually on the basis of energy, spin, parity, one-nucleon transfer reaction data (if they exist), decay properties, and wave functions.

The main components of the wave functions of some low-lying states in ^{66}Ga and ^{70}As are shown in Tables 2 and 3, respectively. Usually the wave functions are very complex. There are states, which have more than six hundred components. Nevertheless, in some cases the states are dominated by only one proton-neutron multiplet. Thus it is worth to compare the experimental and IBFFM energy spectra also with the predictions of the parabolic rule (Figs.6 and 7).

The $\pi \tilde{p}_{3/2} \nu \tilde{f}_{5/2}$ multiplet. As an example, let us discuss the energy splitting of the $\pi \tilde{p}_{3/2} \nu \tilde{f}_{5/2}$ multiplet in $^{66,68,70}\text{Ga}$ and $^{70,72}\text{As}$. The parabolic rule predicts an open-up parabola for the energy splitting in ^{66}Ga and open-down one in ^{68}Ga (Fig.7). This is in accordance with the experimental facts, because the 1^+ , 2^+ , 3^+ , and 4^+ states of the multiplet can be identified with the 44 and 109 keV $1_1^+ + 1_2^+$, 66 keV 2_1^+ , 162 keV 3_1^+ , and 415 keV 4_1^+ states in ^{66}Ga and 0 keV 1_1^+ , 175 keV 2_1^+ , 376 and 676 keV $3_1^+ + 3_2^+$, and 496 keV 4_1^+ states in ^{68}Ga (Figs.9 and 11). The IBFFM calculations are in accordance with the classification of the parabolic rule, because the $1_1^+ + 1_2^+$, 2_1^+ , 3_1^+ , and 4_1^+ states in ^{66}Ga , as well as 1_1^+ , 2_1^+ , $3_1^+ + 3_2^+$, and 4_1^+ states in ^{68}Ga have dominating (or at least very strong) $\pi \tilde{p}_{3/2} \nu \tilde{f}_{5/2}$ components. The inversion of parabola is connected with the fact, that the $\tilde{f}_{5/2}$ neutron is particle-like in $^{66}\text{Ga}_{35}$ ($V^2 > 0.5$) and hole-like in $^{68}\text{Ga}_{37}$ ($V^2 > 0.5$).

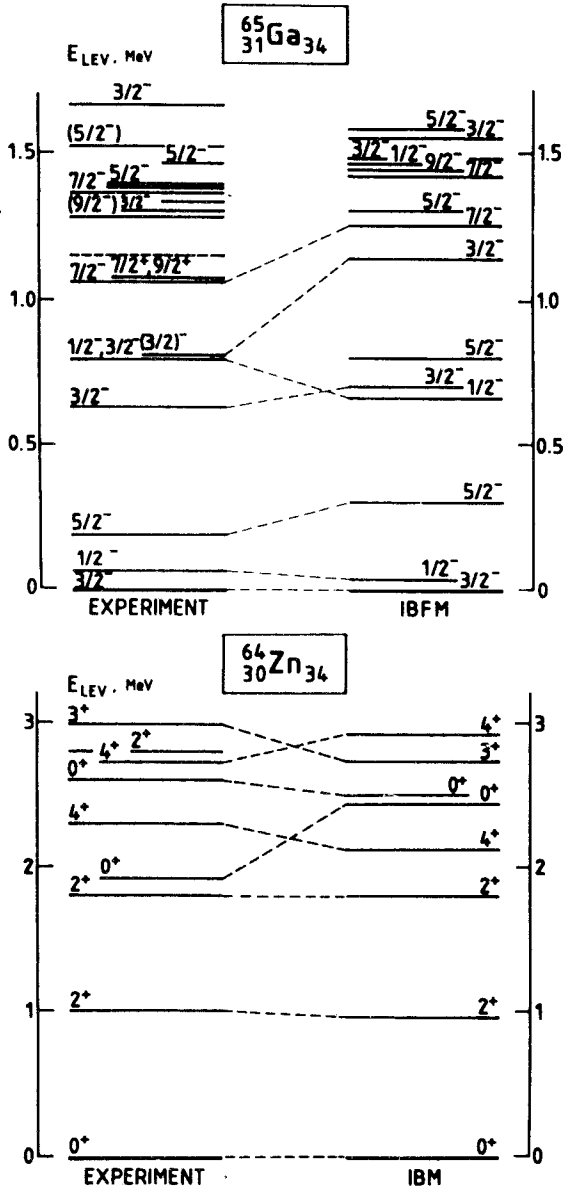


Fig.8. Experimental energy spectra of ^{64}Zn [30] and ^{65}Ga [31] and the corresponding theoretical IBM and IBFM results [4]

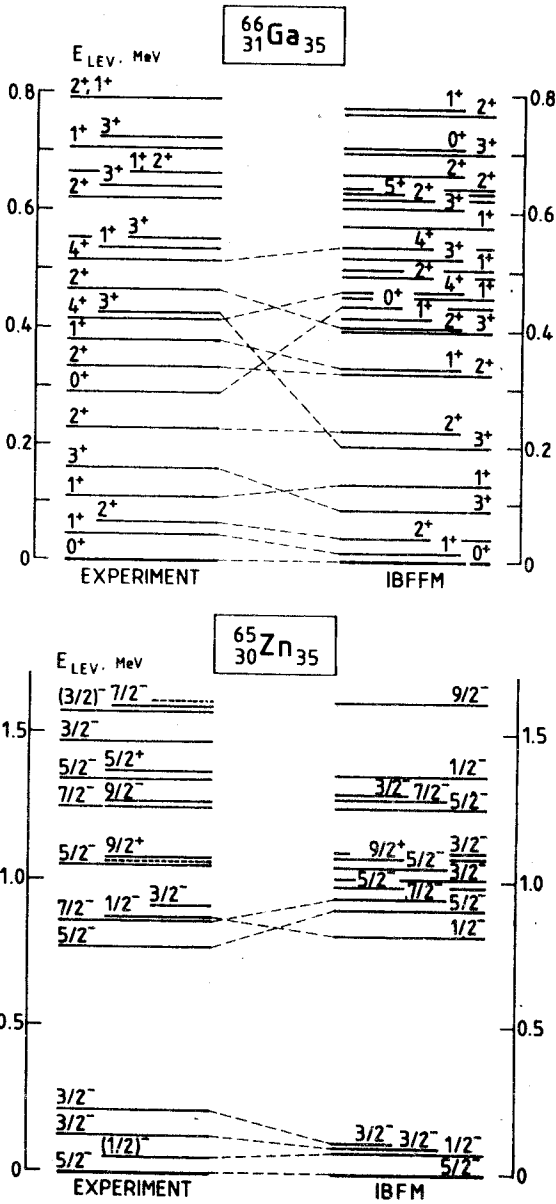


Fig.9. Experimental energy spectra of ^{65}Zn [31] and ^{66}Ga [4] and the corresponding theoretical IBFM and IBFFM results [4]

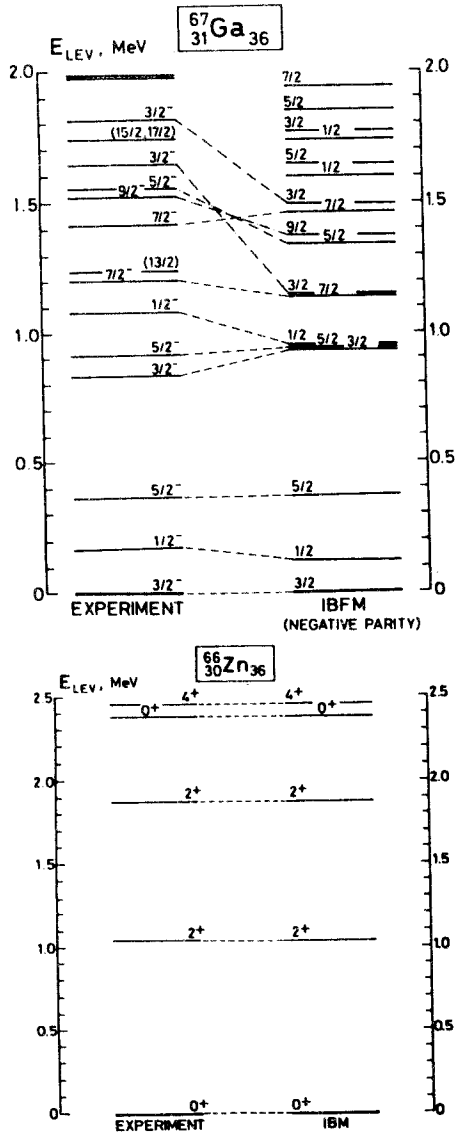


Fig.10. Experimental energy spectra of ^{66}Zn [30] and ^{67}Ga [32] and the corresponding theoretical IBM and IBFM results [5,6]. --- sign shows the assignment of the theoretical levels to the experimental ones. If the assignment is made on the basis of energies only, it is marked by -.-.-

Table 2. Main components ($\geq 4\%$) in the IBFFM wave functions of some low-lying states in ^{66}Ga . The basis states are $|j_\pi j_\nu\rangle j_\pi j_\nu, n_d I; J\rangle$ (see the text). The last column displays the corresponding amplitudes in the wave functions

J^π	(j_π, j_ν)	$j_\pi j_\nu, n_d I$	A	J^π	(j_π, j_ν)	$j_\pi j_\nu, n_d I$	A	
0_1^+	(3/2, 5/2)	2;12	0.62	2_2^+	(3/2, 5/2)	2;00	0.35	
	(3/2, 3/2)	0;00	0.23		(3/2, 3/2)	2;00	0.45	
	(3/2, 3/2)	2;12	0.43		(3/2, 5/2)	3;12	-0.24	
	(1/2, 5/2)	2;12	-0.26		(3/2, 3/2)	3;12	-0.41	
	(1/2, 3/2)	2;12	0.30		0_2^+	(3/2, 3/2)	0;00	0.36
	(3/2, 5/2)	2;32	-0.22			(1/2, 1/2)	0;00	-0.25
1_1^+	(3/2, 5/2)	1;00	0.54	(5/2, 5/2)	0;00	-0.53		
	(3/2, 5/2)	1;20	-0.24	(5/2, 5/2)	0;20	0.28		
	(3/2, 3/2)	2;12	0.31	(3/2, 5/2)	2;12	-0.43		
	(1/2, 5/2)	2;12	0.24	(1/2, 3/2)	2;12	0.21		
	(3/2, 5/2)	3;12	0.41	4_1^+	(1/2, 5/2)	3;12	-0.21	
	(3/2, 3/2)	3;12	-0.23		(3/2, 5/2)	4;00	0.62	
2_1^+	(3/2, 5/2)	2;00	0.62	(5/2, 5/2)	4;00	0.37		
	(1/2, 5/2)	2;00	-0.25	(3/2, 5/2)	4;20	-0.26		
	(3/2, 5/2)	2;12	-0.23	(5/2, 5/2)	5;12	0.39		
	(3/2, 5/2)	2;20	-0.27	5_1^-	(1/2, 9/2)	5;00	0.63	
	(1/2, 5/2)	3;12	-0.27		(5/2, 9/2)	5;00	-0.38	
	(5/2, 5/2)	4;12	-0.26	(1/2, 9/2)	5;20	-0.30		
1_2^+	(3/2, 5/2)	1;00	0.51	(5/2, 9/2)	7;12	0.35		
	(3/2, 5/2)	1;20	-0.21	7_1^-	(1/2, 9/2)	5;12	0.32	
	(3/2, 5/2)	2;12	0.30		(5/2, 9/2)	7;00	0.74	
	(3/2, 3/2)	2;12	-0.24	(5/2, 9/2)	7;12	-0.26		
	(1/2, 3/2)	2;12	-0.26	(5/2, 9/2)	7;20	-0.39		
	(3/2, 3/2)	3;12	0.33					
3_1^+	(3/2, 5/2)	3;00	-0.46					
	(3/2, 3/2)	3;00	0.20					
	(1/2, 5/2)	3;00	0.50					
	(1/2, 5/2)	3;20	-0.23					
	(5/2, 5/2)	5;12	0.43					

Table 3. Wave functions of some low-lying states of ^{70}As . Only the strongest components are given. The basis states are $| (j_{\pi} j_{\nu}) j_{\pi\nu}, n_d I; J \rangle$ (see in text)

J^{π}	(j_{π}, j_{ν})	$j_{\pi\nu}; n_d I$	$ A $	J^{π}	(j_{π}, j_{ν})	$j_{\pi\nu}; n_d I$	$ A $
0_1^+	(5/2,5/2)	0;00	0.83	3_4^+	(3/2,5/2)	3;00	0.79
0_2^+	(1/2,1/2)	0;00	0.70	4_1^+	(5/2,5/2)	4;00	0.77
1_1^+	(3/2,5/2)	1;00	0.73	4_2^+	(3/2,5/2)	4;00	0.56
1_2^+	(5/2,5/2)	1;00	0.66		(5/2,5/2)	5;12	0.48
1_3^+	(1/2,1/2)	1;00	0.66	2_1^-	(5/2,9/2)	2;00	0.76
2_1^+	(5/2,5/2)	2;00	0.51	3_1^-	(5/2,9/2)	3;00	0.75
	(1/2,5/2)	2;00	0.45	4_1^-	(1/2,9/2)	4;00	0.52
2_2^+	(5/2,5/2)	2;00	0.56		(5/2,9/2)	4;00	0.41
	(3/2,5/2)	2;00	0.41	4_2^-	(5/2,9/2)	4;00	0.65
2_3^+	(5/2,1/2)	2;00	0.63	5_1^-	(5/2,9/2)	5;00	0.56
3_1^+	(1/2,5/2)	3;00	0.51		(1/2,9/2)	5;00	0.49
	(5/2,5/2)	3;00	0.48	6_1^-	(5/2,9/2)	6;00	0.70
3_2^+	(5/2,5/2)	3;00	0.63	7_1^-	(5/2,9/2)	7;00	0.75
3_3^+	(5/2,1/2)	3;00	0.78				

The $\pi \tilde{p}_{3/2} \nu \tilde{f}_{5/2}$ multiplet is seen in ^{70}Ga also, and the energy splitting exhibits an open-down parabola, in accordance with the prediction of the parabolic rule [7].

The members of the multiplet $\pi \tilde{p}_{3/2} \nu \tilde{f}_{5/2}$ in ^{70}As are fragmented into different states. Nevertheless in the 1_1^+ , 3_4^+ , and 4_2^+ states the $\pi \tilde{p}_{3/2} \nu \tilde{f}_{5/2}$ components are dominating (Table 3).

On the basis of lifetime measurements and other considerations Hübner [44] came to the conclusion that the 1_1^+ state of ^{72}As has either the $\pi p_{3/2}^{-1} \nu f_{5/2}^{-1}$ or $\pi p_{3/2}^{-1} \nu p_{1/2}$ configuration. The IBFFM calculations give $\pi \tilde{p}_{3/2} \nu \tilde{f}_{5/2}$ as the dominating configuration for this state. The parabolic rule predicts an open-down parabola for energy splitting of the $\pi \tilde{p}_{3/2} \nu \tilde{f}_{5/2}$ multiplet, with a minimum energy for the 1^+ state. The 4^+ member of this multiplet may be the 4_1 state.

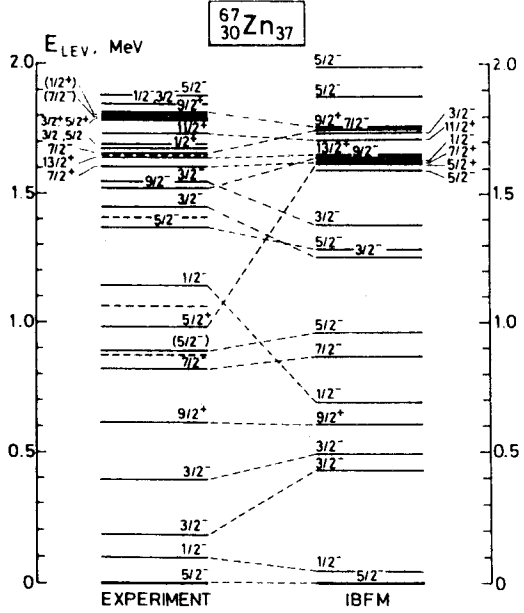
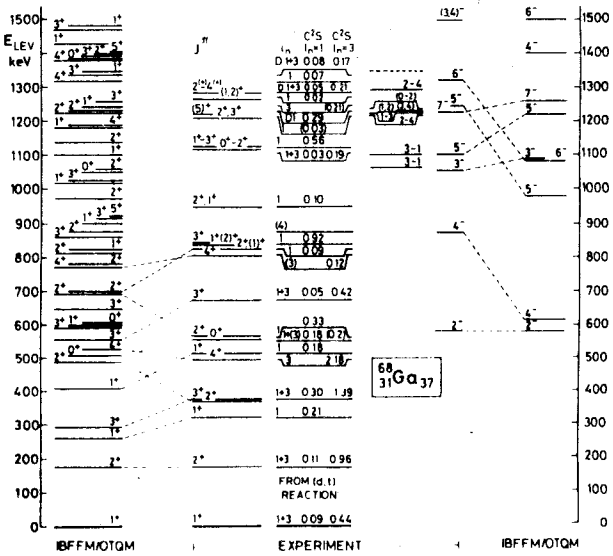


Fig.11. Experimental energy spectra of ^{67}Zn [32] and ^{68}Ga [5,6] and the corresponding theoretical IBFM and IBFFM results [5,6]. The (d, t) reaction data were taken from Daehnick et al. [33]. See also caption of Fig.10

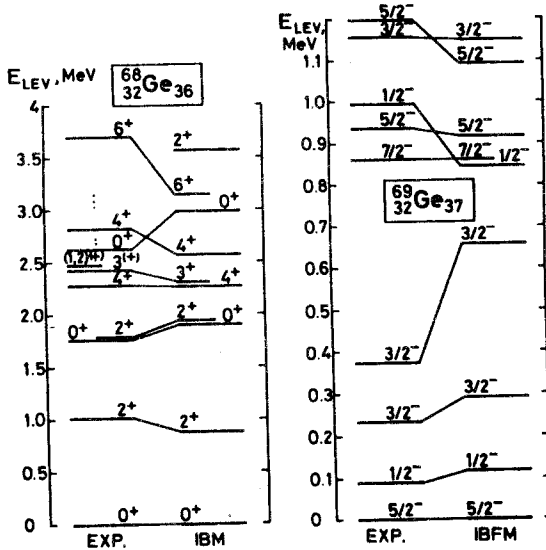
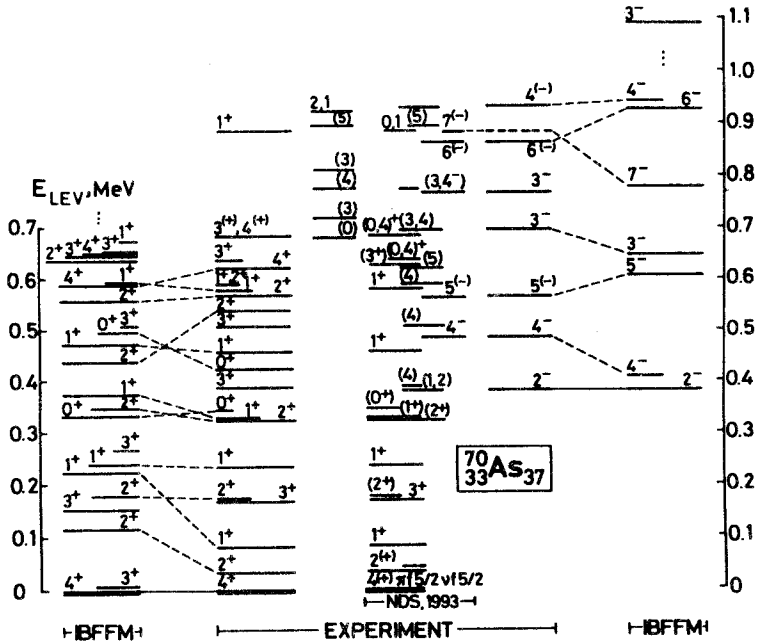


Fig.12. Experimental energy spectra of ^{68}Ge [34], ^{69}Ge [35], and ^{70}As [8,36] and the corresponding theoretical IBM and IBFFM results [8]

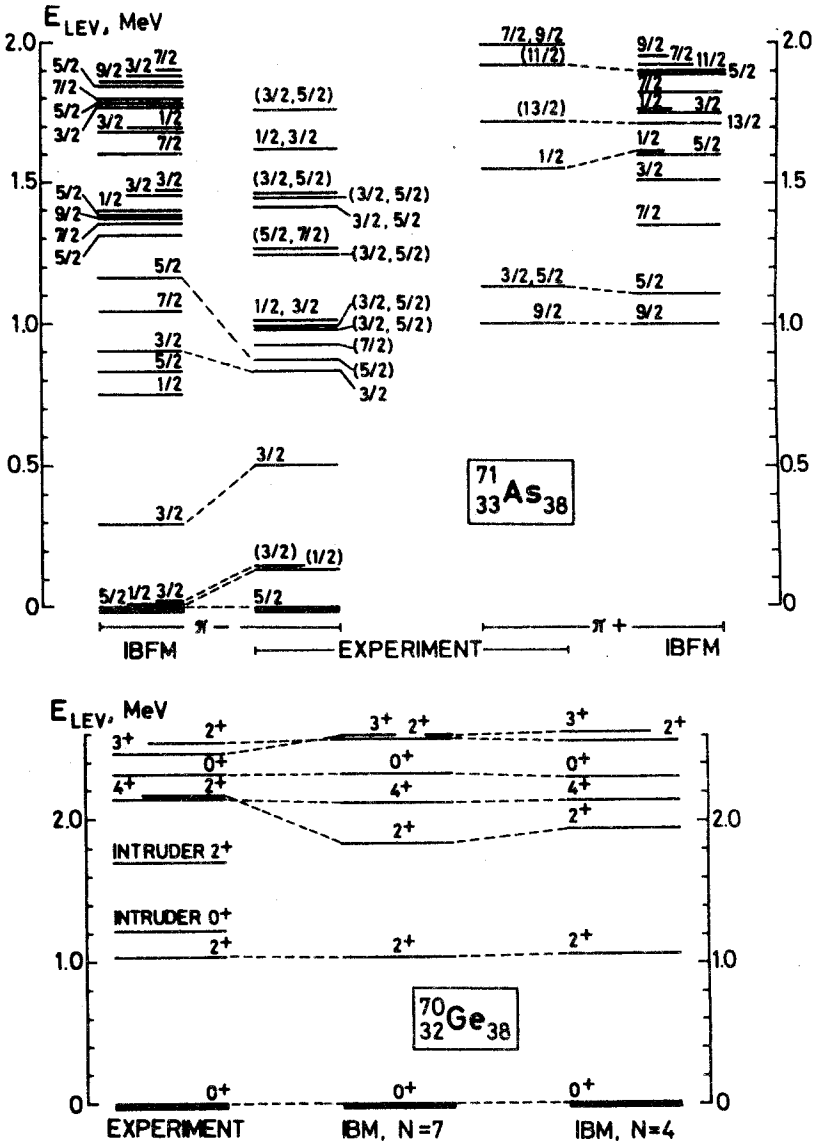


Fig.13. Experimental energy spectra of ^{70}Ge [36] and ^{71}As [37] and the corresponding theoretical IBM and IBFM results [9,13]. $\pi+$ and $\pi-$ mean positive and negative parity states, respectively

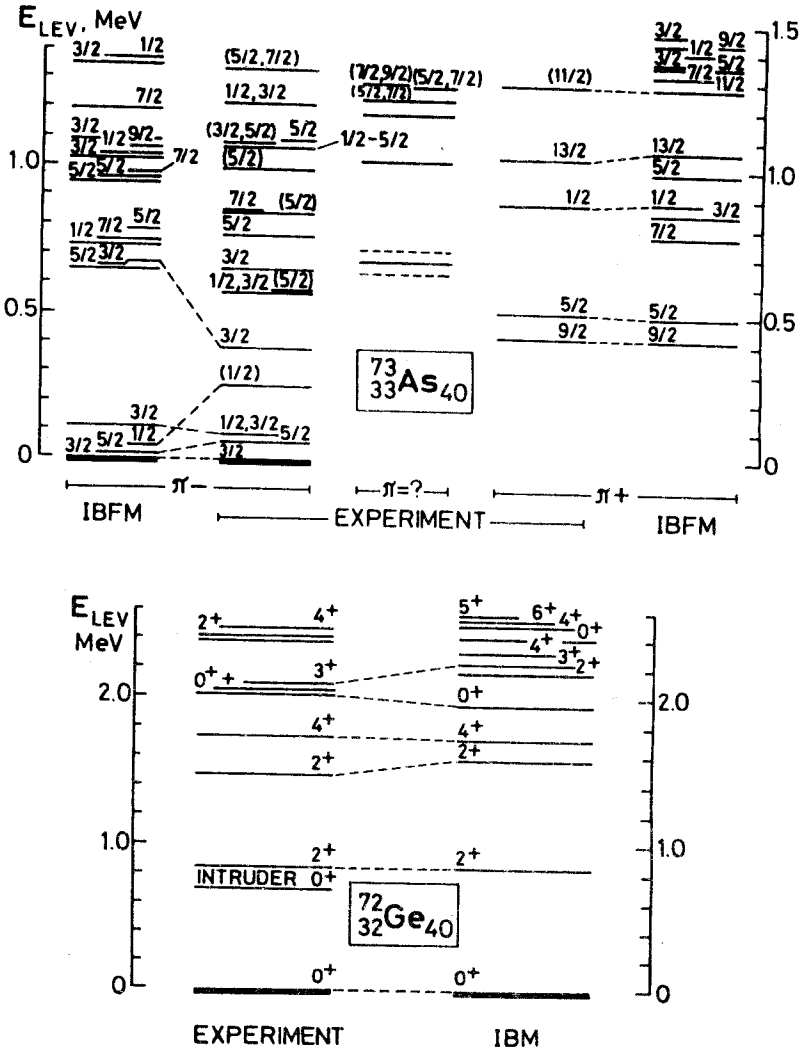


Fig.15. Experimental energy spectra of ^{72}Ge [39] and ^{73}As [40,10] and the corresponding theoretical IBM and IBFM results [11,13]

The 2^+ and 3^+ members are fragmented into different states (e.g., 2_1^+ , 2_2^+ , etc., see Table IX in [9]).

The $\pi \tilde{p}_{3/2} \nu \tilde{p}_{1/2}$ doublet. In the case of doublets, for example in $\pi \tilde{p}_{3/2} \nu \tilde{p}_{1/2}$, the energy splitting does not depend on occupation probability, so the shape of splitting of the given multiplet is very similar for all investigated nuclei (see

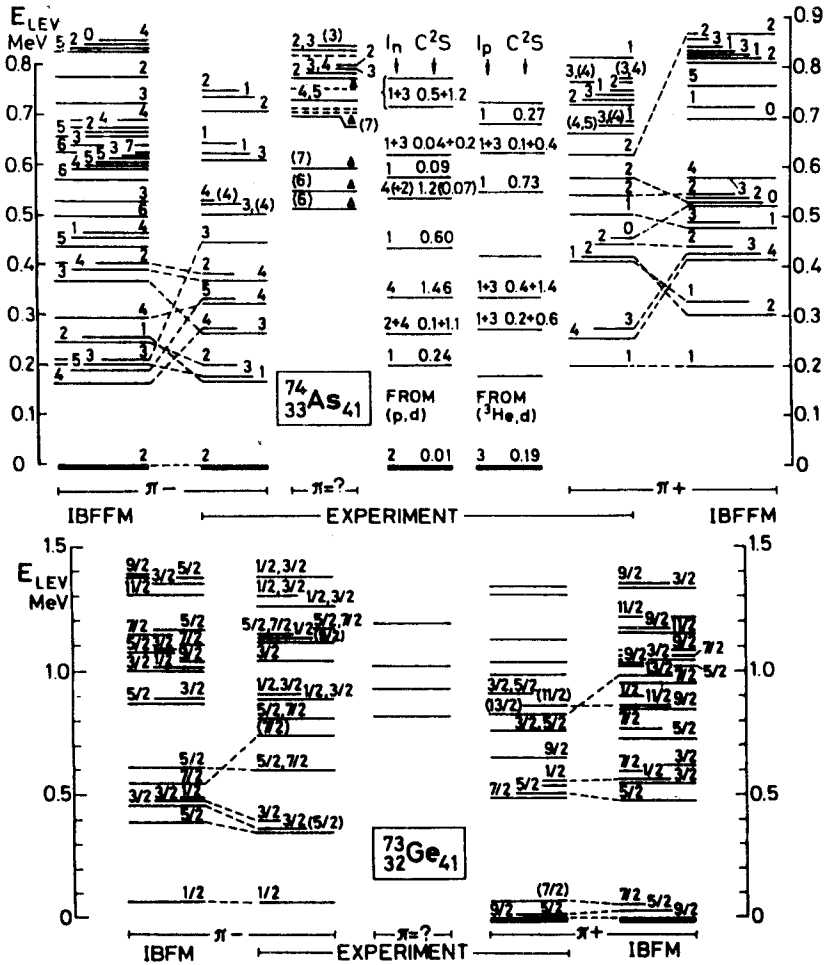


Fig.16. Experimental energy spectra of ^{73}Ge [40] and ^{74}As [11,13] and the corresponding theoretical IBFM and IBFFM results [11,13]. ^{74}As levels, marked with Δ , were taken from García Bermúdez et al. [41]; the (p, d) and $(^3\text{He}, d)$ results from Fournier et al. [42] and Rosner et al. [43], respectively

Fig.7). The 1^+ and 2^+ members of the $\pi \tilde{p}_{3/2} \tilde{v}_{1/2}$ doublet are well seen in ^{70}Ga [7] and ^{74}As [11]. In both cases $E(1^+) < E(2^+)$, in accordance with the predictions of the parabolic rule and IBFFM calculations (for ^{74}As ; see 1_1^+ and 2_1^+ states in Fig.17).

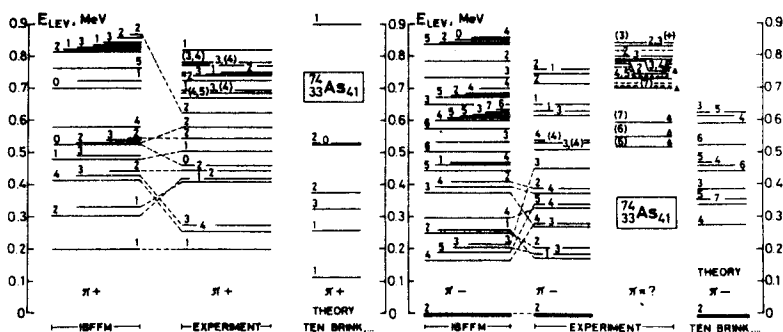


Fig.17. Level scheme of ^{74}As [11] compared with the present IBFFM and previous calculations by B.O.Ten Brink et al. [51]. The levels, marked with triangle, were observed in [41] from $(\alpha, n\gamma)$ reaction

Some members of the $\pi \tilde{f}_{5/2} \nu \tilde{f}_{5/2}$ multiplet were identified in ^{70}As and ^{72}As .

According to the parabolic rule the lowest-lying 0^+ states in ^{70}As are expected to be relatively pure, and they belong to the $\pi \tilde{f}_{5/2} \nu \tilde{f}_{5/2}$ and/or $\pi \tilde{p}_{1/2} \nu \tilde{p}_{1/2}$ quasiparticle multiplets. Many low-lying 1^+ levels are expected and a strong configuration mixing among them. The same is true for the 2^+ and 3^+ states. The lowest-lying 4^+ state belongs to the $\pi \tilde{f}_{5/2} \nu \tilde{f}_{5/2}$ multiplet, and it is probably well separated from the 4^+ members of the $\pi \tilde{p}_{3/2} \nu \tilde{f}_{5/2}$ and $\pi \tilde{f}_{5/2} \nu \tilde{p}_{3/2}$ multiplets.

The IBFFM calculations (Fig.12 and Table 3) show, that the 0^+_1 345 keV and 4^+_1 ground states of ^{70}As have $\pi \tilde{f}_{5/2} \nu \tilde{f}_{5/2}$ as dominating configurations. The $\pi \tilde{f}_{5/2} \nu \tilde{f}_{5/2}$ components are fragmented in the 1^+_1 , 1^+_2 , 2^+_1 , 2^+_2 , 3^+_1 , 3^+_2 states with other components. The 0^+_1 state decays by a strong M1 transition to the 1^+_1 state, as expected. The low-lying 5^+ member of the $\pi \tilde{f}_{5/2} \nu \tilde{f}_{5/2}$ multiplet is missing in the experimental spectrum.

According to Bertschat et al. [45] the best agreement between the predicted and measured g -factors of the 3^+_1 state at 214 keV in ^{72}As is obtained, if one assumes the $\pi f_{5/2} \nu f_{5/2}^{-1}$ and $\pi f_{5/2} \nu p_{1/2}$ configurations. Our IBFFM calculations indicate mixed configuration for this state, with $\pi \tilde{f}_{5/2} \nu \tilde{f}_{5/2}$ configuration being

the strongest one. The parabolic rule predicts an open-up parabola for the splitting of the multiplet, with a minimum energy for the 3^+ (or 4^+) member.

Some members of the $\pi \tilde{f}_{5/2} \nu \tilde{g}_{9/2}$ multiplet were observed almost in all investigated odd-odd Ga and As nuclei.

On the basis of the parabolic rule we may expect that the 2_1^- , 3_1^- , 6_1^- , and 7_1^- states in ^{70}As are relatively pure and belong very likely to the $\pi \tilde{f}_{5/2} \nu \tilde{g}_{9/2}$ multiplet (see Fig.6). In the low-lying 4_1^- and 5_1^- states there is probably a stronger configuration mixing. As Fig.12 shows, the low-lying negative parity states of ^{70}As have been reasonably well reproduced by the IBFFM calculations. The 2_1^- , 3_1^- , 6_1^- , and 7_1^- levels are rather pure and belong mainly to the $\pi \tilde{f}_{5/2} \nu \tilde{g}_{9/2}$ multiplet (Table 3). The 699 keV 3_1^- level decays by M1 transition to the 2_1^- state, in accordance with expectation for the neighbouring members of the same multiplet. The 4_1^- , 4_2^- , and 5_1^- states have mixed $\pi \tilde{p}_{1/2} \nu \tilde{g}_{9/2}$ and $\pi \tilde{f}_{5/2} \nu \tilde{g}_{9/2}$ multiplets as the main configurations.

According to the parabolic rule the energy splitting of the $\pi \tilde{f}_{5/2} \nu \tilde{g}_{9/2}$ multiplet shows an open-down parabola with a minimum energy for the 2^- state in ^{72}As , too. On the basis of magnetic dipole moment measurement by Hogervorst et al. [46] one may conclude that the 2^- ground state of ^{72}As has predominantly a $\pi \tilde{f}_{5/2} \nu \tilde{g}_{9/2}$ configuration. The IBFFM calculations confirm these results: in the 2_1^- ground, 3_1^- and 7_1^- states the dominating configuration is $\pi \tilde{f}_{5/2} \nu \tilde{g}_{9/2}$ (Table IX in [9]). In a recent publication, Döring et al. [47] assigned to the 562.8 keV level 7^- spin and parity (instead of the former assignment (6)). This state may be the 7^- member of the $\pi \tilde{f}_{5/2} \nu \tilde{g}_{9/2}$ multiplet (Fig.14).

The 2^- and 7^- members of the $\pi \tilde{f}_{5/2} \nu \tilde{g}_{9/2}$ multiplet could be identified also in ^{68}Ga (Fig.11 and [6]), ^{70}Ga [7]; and the 2^- member in ^{74}As (Fig.16 and [11]).

The 4^- and 5^- members of the $\pi \tilde{p}_{1/2} \nu \tilde{g}_{9/2}$ doublet were seen in ^{68}Ga [5,6], ^{70}As [8] and ^{72}As [9], although they are mixed with other components. According to the parabolic rule $E(4^-) < E(5^-)$ (see Figs.6 and 7), in agreement with the experimental data and IBFFM calculations (Fig.11 for ^{68}Ga , Fig.12 and Table 3 for ^{70}As , and Fig.14 and Table IX in [9] for ^{72}As).

In the low-lying 5^- and 6^- states components of the $\pi \tilde{p}_{3/2} \nu \tilde{g}_{9/2}$ multiplet were seen in ^{68}Ga (Fig.11 and [5,6]) and ^{70}Ga [7].

Table 4. *d*-boson composition of the IBFFM wave functions of some low-lying states in ^{66}Ga

J_k^π	n_d				
	0	1	2	3	4
0_1^+	0.065	0.750	0.072	0.110	0.003
1_1^+	0.344	0.466	0.121	0.065	0.004
2_1^+	0.502	0.282	0.172	0.038	0.006
1_2^+	0.339	0.460	0.132	0.064	0.005
3_1^+	0.504	0.303	0.146	0.043	0.004
2_2^+	0.381	0.396	0.163	0.054	0.006
0_2^+	0.473	0.313	0.168	0.040	0.006

For each state J_k^π , the numbers in the Table present the value of $\sum_{j_\pi j_\nu} \xi^2[(j_\pi j_\nu) j_{\pi\nu}, n_d l; J]$ for each of possible values of *d*-boson number: $n_d = 0, 1, 2, \dots, N$.

The *d*-boson composition of the IBFFM wave functions of some low-lying states in ^{66}Ga is given in Table 4. The 0_1^+ ground state of ^{66}Ga is basically of one-*d*-boson type. The total contribution of sizeable one-*d*-boson components is 75%. We note that this is an effect of boson-fermion interaction, similar to the $j-1$ anomaly, which was studied previously in the cluster-vibration model for odd-even nuclei [48] and appears also in IBFM for odd-even nuclei [24].

The low-lying triplet of ^{73}Ge positive-parity levels, $9/2^+$, $5/2^+$, and $7/2^+$ (see Fig.16) is associated also with the $J=j-1, j-2$ anomaly due to lowering of $|\tilde{g}_{9/2}, 12; 5/2\rangle$ and $|\tilde{g}_{9/2}, 12; 7/2\rangle$ one-*d*-boson multiplet states. The $5/2^+$ lowering is produced by the dynamical quadrupole interaction (and admixture of $d_{5/2}$ configuration from the shell above), while the $7/2^+$ lowering is due to the exchange interaction.

The *electromagnetic moments* and the corresponding IB(FF)M results are given in Table 5. Here we present calculated moments only for those states which have at least one experimentally measured moment (either electric quadrupole or magnetic dipole).

Table 5. Experimental electric quadrupole (Q) and magnetic dipole (μ) moments of Zn, Ga, Ge, and As nuclei compared with IB(FF)M theoretical results

Nucleus	J^π	E , keV	Q(eb)		$\mu(\mu_N)$			Main config.
			Exp. [49]	Calc. Ref.	Exp. [49]	Calc. Ref.		
$^{64}_{30}\text{Zn}_{34}$	2^+_1	992	-0.124(12) -0.143(21)	-0.07	+0.84(18) +0.92(20)	+0.94	One d -boson	
$^{65}_{30}\text{Zn}_{35}$	$5/2^-_1$	0	-0.023(2) ^u	-0.003	+0.7690(2)	a)+1.38 b)+0.84	$v\tilde{f}5/2$	
	$3/2^-_1$	115		+0.10	-0.78(20)	a)-1.49 b)-0.82	$v\tilde{p}3/2$	
	$3/2^-_2$	207		-0.06 [4]	+0.73(25)	a)+0.52 b)+0.43 [4]	$v\tilde{f}5/2\otimes 2^+$	
	$9/2^+_1$	1066			-1.73(49)	a)-1.80 b)-1.03	$v\tilde{g}9/2$	
$^{66}_{31}\text{Ga}_{35}$	2^+_1	66		-0.15	$\pm 1.011(18)^h$	a)+1.03 b)+0.72	$\pi\tilde{p}3/2v\tilde{f}5/2$	
	7^-_1	1464	$\pm 0.78(4)^{st}$	-0.40	+0.903(21)	a)-0.06 b)+0.70	$\pi\tilde{f}5/2v\tilde{g}9/2$	
	9^+_1	3043		-0.35	$\pm 4.23(90)$	a)+5.12 b)+4.59		
$^{66}_{30}\text{Zn}_{36}$	2^+_1	1039		-0.064	+0.94(22)	+0.91	One d - boson	
$^{67}_{30}\text{Zn}_{37}$	$5/2^-_1$	0	+0.150(15) ^u	+0.07	+0.8754790(84)	+1.35	$v\tilde{f}5/2$	
	$1/2^-_1$	93			+0.587(11)	+0.72	$v\tilde{p}1/2$	
	$3/2^-_1$	185		-0.04 [6]	+0.50(6)	+0.13 [6]	$v\tilde{f}5/2\otimes 2^+$	
	$9/2^+_1$	604	$\approx \pm 0.3[32]$	-0.20	-1.097(9)	-1.02	$v\tilde{g}9/2$	
$^{67}_{31}\text{Ga}_{36}$	$3/2^-_1$	0	$\pm 0.195^{st}$	+0.07	+1.8507(3)	+2.08	$\pi\tilde{p}3/2$	
$^{68}_{31}\text{Ga}_{37}$	1^+_1	0	$\pm 0.0277(14)^{k, st}$	+0.0082	$\pm 0.01175(5)^k$	-0.0134	$\pi\tilde{p}3/2v\tilde{f}5/2$	
	7^-_1	1230	$\pm 0.72(2)^{st}$	-0.514	+0.707(14)	+0.67	$\pi\tilde{f}5/2v\tilde{g}9/2$	
$^{69}_{32}\text{Ge}_{37}$	$5/2^-_1$	0	$\pm 0.024(5)^{st}$	+0.04	$\pm 0.735(7)$	0.73	$v\tilde{f}5/2$	

Nucleus	J^π	E , keV	Q(eb)			$\mu(\mu_N)$			Main config.
			Exp. [49]	Calc.	Ref.	Exp. [49]	Calc.	Ref.	
$^{70}_{33}\text{As}_{37}$	4^+_1	0	+0.094(24)	-0.023	[8]	+2.1061(2)	+2.1	[8]	$\pi\tilde{f}5/2\nu\tilde{f}5/2$
	7^-_1	888				+0.75(5) [50]	+0.77		$\pi\tilde{f}5/2\nu\tilde{g}9/2$
$^{70}_{32}\text{Ge}_{38}$	2^+_1	1039	+0.03(6) or +0.09(6)	-0.197		+0.936(52)	+0.914		One <i>d</i> -boson
$^{71}_{32}\text{Ge}_{39}$	$1/2^-_1$	0				+0.547(5)	+0.445		$\nu\tilde{p}1/2$
	$5/2^-_1$	175				+1.018(10)	+0.987		$\nu\tilde{f}5/2$
	$9/2^+_1$	199	$\pm 0.34(5)$	-0.230	[9]	-1.0413(7)	-1.221	[9]	$\nu\tilde{g}9/2$
$^{71}_{33}\text{As}_{38}$	$5/2^-_1$	0	-0.021(6)	-0.156		(+)1.6735(18)	+1.010		$\pi\tilde{f}5/2$
	$9/2^+_1$	1001		-0.365		+5.15(9)	+5.985		$\pi\tilde{g}9/2$
$^{72}_{33}\text{As}_{39}$	2^-_1	0	-0.082(24)	-0.132		-2.1566(3)	-1.809		$\pi\tilde{f}5/2\nu\tilde{g}9/2$
	3^+_1	214		+0.229		+1.580(18) ^h	+1.525		$\pi\tilde{f}5/2\nu\tilde{f}5/2$
$^{72}_{32}\text{Ge}_{40}$	2^+_1	834	-0.13(6)	-0.209		+0.798(66)	+0.888		One <i>d</i> - boson
$^{73}_{32}\text{Ge}_{41}$	$9/2^+_1$	0	-0.173(26) ^u	-0.165		-0.8794677(2)	-1.204		$\nu\tilde{g}9/2$
	$5/2^+_1$	13	-0.4(3) or +0.22 [58]	+0.230		-0.0941(25)	-1.091		
$^{73}_{33}\text{As}_{40}$	$5/2^-_1$	67		-0.112	[11]	+1.63(10)	+0.964	[11]	$\pi\tilde{f}5/2$
	$9/2^+_1$	428		-0.392		+5.234(14)	+5.955		$\pi\tilde{g}9/2$
$^{74}_{33}\text{As}_{41}$	2^-_1	0		+0.111		-1.597(3)	-1.393		$\pi\tilde{f}5/2\nu\tilde{g}9/2$
	4^+_1	259		+0.417		+3.238(40)	+3.793		$\pi\tilde{p}3/2\nu\tilde{f}5/2$

a) $g_s^v = 0.9g_s^v$ (free), b) $g_s^v = 0.5g_s^v$ (free)

h) does not include Knight-shift correction

k) $\mu / Q < 0$ (signs of μ and Q are different)

st) «Sternheimer» or other polarization correction included

u) no polarization correction included

As Table 5 shows, the signs of moments were correctly reproduced in 37 cases of the total 39. (The exceptions are the electric quadrupole moments of $^{70}\text{As } 4^+_1$ and $^{70}\text{Ge } 2^+_1$ states). In 11 cases the signs of moments were not determined experimentally. The calculations gave definite predictions for signs, and allowed one to predict more than 200 moments which were not measured up to now (see Refs. [4,9,11]).

The calculated and available experimental B(E2), B(M1) *reduced transition probabilities and γ -branching ratios* for ^{68}Ga transitions are given in Table 6. Similar data have been obtained also for ^{66}Ga [4], ^{72}As [9], and ^{74}As [11] transitions. As Table 6 shows, there is a reasonable agreement between theory and experiment, at least all leading branches are correctly reproduced. The γ -transition probabilities depend critically even on weak components of the wave function; we note a disagreement for the $3_1^+ \rightarrow 1_1^+$ transition.

Table 6. Calculated E2 and M1 transitions between the low-lying levels in ^{68}Ga and comparison with available data. The assignment of calculated to experimental levels is according to Fig.11

$J_i^\pi \rightarrow J_f^\pi$	10^2 B(E2) (e^2b^2)		10 B(M1) (μ_N^2)		I_γ	
	IBFFM	Exp. [34]	IBFFM	Exp. [34]	IBFFM	Exp. [34]
$2_1^+ \rightarrow 1_1^+$	0.13		1.822	≥ 0.014	100	100
$1_2^+ \rightarrow 2_1^+$	0.03		0.130		5.5	5.5
$\rightarrow 1_1^+$	0.04		0.221		100	100
$2_2^+ \rightarrow 1_2^+$	0.25		0.024		0.1	
$\rightarrow 2_1^+$	0.002		0.044		11.9	3.0
$\rightarrow 1_1^+$	0.00006		0.056		100	100
$3_1^+ \rightarrow 2_2^+$	0.01		0.008		10^{-7}	
$\rightarrow 1_2^+$	0.0004				10^{-7}	
$\rightarrow 2_1^+$	0.44		1.593	≥ 0.005	100	100
$\rightarrow 1_1^+$	0.03	≥ 0.05			0.1	45
$4_1^+ \rightarrow 3_1^+$	0.40		1.389	≥ 0.038	100	100
$\rightarrow 2_2^+$	0.01				0.0008	
$\rightarrow 2_1^+$	0.03	> 0.01			0.3	4.6
$1_3^+ \rightarrow 3_1^+$	0.09				0.006	
$\rightarrow 2_2^+$	0.48		0.050		2.6	4.2
$\rightarrow 1_2^+$	0.23		0.036		5.0	1.0
$\rightarrow 2_1^+$	0.03		0.134		100	100
$\rightarrow 1_1^+$	0.002		0.004		10.5	20

$J_i^\pi \rightarrow J_f^\pi$	$10^2 B(E2) (e^2b^2)$		$10 B(M1) (\mu_N^2)$		I_γ	
	IBFFM	Exp. [34]	IBFFM	Exp. [34]	IBFFM	Exp. [34]
$0_1^+ \rightarrow 1_3^+$			0.217		0.08	
$\rightarrow 2_2^+$	0.02				0.001	
$\rightarrow 1_2^+$			0.925		60	15
$\rightarrow 2_1^+$	1.01				2.8	
$\rightarrow 1_1^+$			0.116		100	100
$2_3^+ \rightarrow 0_1^+$	0.00007				3×10^{-12}	
$\rightarrow 1_3^+$	0.08		0.009		0.01	
$\rightarrow 4_1^+$	0.004				5×10^{-6}	
$\rightarrow 3_1^+$	0.23		0.271		21	0.9
$\rightarrow 2_2^+$	0.04		0.444		35	5.0
$\rightarrow 1_2^+$	0.005		0.050		8.3	5.8
$\rightarrow 2_1^+$	1.34		0.0003		9.8	13.4
$\rightarrow 1_1^+$	0.20		0.044		100	100
$3_2^+ \rightarrow 2_3^+$	0.12		0.377		0.7	
$\rightarrow 1_3^+$	0.25				0.003	
$\rightarrow 4_1^+$	0.22		0.00002		0.004	
$\rightarrow 3_1^+$	0.19		0.0003		0.1	9.3
$\rightarrow 2_2^+$	0.05		0.065		2.5	
$\rightarrow 1_2^+$	0.09				0.05	
$\rightarrow 2_1^+$	0.19		0.561		100	100
$\rightarrow 1_1^+$	0.04				0.6	2.8
$4_2^+ \rightarrow 3_2^+$	1.06		0.167		2.1	
$\rightarrow 2_3^+$	0.01				0.003	
$\rightarrow 4_1^+$	0.06		0.583	≥ 0.0014	100	100
$\rightarrow 3_1^+$	0.58		0.257	≥ 0.0004	121	90
$\rightarrow 2_2^+$	0.02				0.1	
$\rightarrow 2_1^+$	0.60				24	20

$J_i^\pi \rightarrow J_f^\pi$	$10^2 B(E2) (e^2b^2)$		$10 B(M1) (\mu_N^2)$		I_γ	
	IBFFM	Exp. [34]	IBFFM	Exp. [34]	IBFFM	Exp. [34]
$2_4^+ \rightarrow 4_2^+$	0.32				4×10^{-8}	
$\rightarrow 3_2^+$	0.03		0.009		0.02	
$\rightarrow 2_3^+$	0.26		0.062		0.6	2.4
$\rightarrow 0_1^+$	0.001				0.00005	
$\rightarrow 1_3^+$	0.12		0.034		0.6	
$\rightarrow 4_1^+$	0.21				0.03	
$\rightarrow 3_1^+$	0.66		0.029		1.9	8.6
$\rightarrow 2_2^+$	0.002		0.013		0.6	4.6
$\rightarrow 1_2^+$	0.006		0.032		2.2	10.5
$\rightarrow 2_1^+$	0.0003		0.026		3.8	4.7
$\rightarrow 1_1^+$	0.93		0.291		100	100
$4_1^- \rightarrow 2_1^-$	2.69	≥ 0.21			100	100
$3_1^- \rightarrow 4_1^-$	1.01		1.212		1.1	
$\rightarrow 2_1^-$	2.10		5.934		100	100
$5_2^- \rightarrow 3_1^-$	0.004				10^{-6}	
$\rightarrow 4_1^-$	0.19		0.579		100	100
$7_1^- \rightarrow 5_2^-$	0.21				100	100
$5_1^- \rightarrow 7_1^-$	4.27				10^{-6}	
$\rightarrow 5_2^-$	0.18		0.304		1.2	
$\rightarrow 3_1^-$	1.36				0.03	
$\rightarrow 4_1^-$	0.32		1.533		100	100
$6_1^- \rightarrow 5_1^-$	0.04		0.072		0.06	≤ 17
$\rightarrow 7_1^-$	0.02		0.076		0.1	
$\rightarrow 5_2^-$	0.47		5.019		100	100
$\rightarrow 4_1^-$	0.96				2.2	8

In Table 7 we present the experimental and calculated *spectroscopic factors* for (*d,t*) transfer reaction, populating the low-lying levels in ^{68}Ga [6]. Four levels (the 1_1^+ , 2_1^+ , 2_2^+ + 3_1^+ , and 4_1^+ states) are excited with large spectroscopic factors. According to the calculation, the low-lying 1_1^+ , 2_1^+ , 3_1^+ , and 4_1^+ states have the largest spectroscopic factors, in qualitative agreement with experiment. We have calculated spectroscopic factors for the $^{75}\text{As}(p,d)^{74}\text{As}$ and $^{73}\text{Ge}(^3\text{He},d)^{74}\text{As}$ reactions [11], too.

Table 7. Spectroscopic factors for $^{69}\text{Ga}_{38}(d,t)^{68}\text{Ga}_{37}$ transfer reaction populating the low-lying levels in ^{68}Ga

J^π	C^2S						
	IBFM				Exp. [33]		
IBFFM	$p_{1/2}$	$p_{3/2}$	$f_{5/2}$	$g_{9/2}$	$p_{1/2} + p_{3/2}$	$f_{5/2}$	$g_{9/2}$
1_1^+	0.012	0.003	3.333		0.09	0.44	
2_1^+	0.023	0.002	3.230		0.11	0.96	
1_2^+	0.308	0.015	0.170		0.21		
2_2^+	0.344	0.430	0.063		} 0.30	} 1.39	
3_1^+		0.114	2.772				
4_1^+			3.227			2.18	
1_3^+	0.055	0.283	0.032		0.18		
0_1^+		0.403			0.18	0.2	
2_3^+	0.004	0.210	0.007		0.33		
3_2^+		1.050	0.278		0.05	0.42	
4_2^+			0.438			0.12	
2_4^+	0.005	0.0004	0.178		0.09		
4_1^-				0.094			
3_1^-				0.020			
5_2^-				0.476			
5_1^-				0.003			
6_1^-				0.360			

Summarizing the results: we have described the energy spectra and electromagnetic properties of even-even core isotopes, odd-A neighbours, and odd-odd nuclei in a consistent way. For example in the ^{64}Zn , ^{65}Zn , ^{65}Ga , and ^{66}Ga quartet more than 400 nuclear data (energy levels, moments, reduced transition probabilities, γ -branching ratios, etc.) have been calculated using ≤ 25 (more or less freely fitted) parameters. As the parameters of calculations mostly show only rather small variation for the neighbouring quartets (see Table 1), the method allows consistent description of a larger group of nuclei.

For odd-odd As nuclei a renormalization of parameters was needed, when we added one nucleon to the neighbouring single-odd nuclei. Such renormalization seems to be a consequence of the softness of nuclei in this region. The appearance of an additional nucleon may change the dynamical deformation sizeably.

4.4. Comparison with earlier theoretical calculations. Theoretical interpretation of the structure of the ^{66}Ga and ^{68}Ga nuclei was completely missing before our works [4–6].

Using the number conserving BCS quasi-proton-quasi-neutron model, Ten-Brink et al. [51] have calculated the energy spectra of $^{70,72,74,76}\text{As}$ and electromagnetic properties of $^{70,72}\text{As}$ nuclei. They used a Schiffer force for the effective proton-neutron residual interaction. It was supposed that the odd-odd As nuclei are spherical and the lowest states have the lowest seniority (two). The phonon degrees of freedom were neglected.

Kimura et al. [52] calculated the level spectrum of ^{72}As , using harmonic oscillator wave functions and a proton-neutron residual interaction of the form:

$$V_{pn}(|\mathbf{r}_p - \mathbf{r}_n|) = V_0[(1 - \alpha) + \alpha(\boldsymbol{\sigma}_n \boldsymbol{\sigma}_p)]\delta(|\mathbf{r}_n - \mathbf{r}_p|).$$

In our IB(FF) calculation it was taken into account that

- a) the Zn and Ge core nuclei may have a small effective deformation (the h_2 and h_3 parameters may differ from zero),
- b) the boson degree of freedom is important and cannot be neglected,
- c) the tensor residual interaction may play an important role in the description of some lowest spin states (0^+ , 1^+).

The experimental energy spectrum of ^{74}As is compared with the results of the present IBFFM and former theoretical calculations in Fig.17. There are about 48 experimentally observed states in ^{74}As below 800 keV. The present IBFFM calculations reproduce 46 levels, while the former calculations [51] give only 18 levels. A comparison with the former theoretical results, obtained on ^{72}As , is given in [9]. Many nuclear moments and reduced transition probabilities have been calculated for the first time in our works [9,11].

5. SUPERSYMMETRY IN ^{74}Se , ^{75}Se , ^{73}As AND ^{74}As NUCLEI

Based on the vibrational symmetry limit of the interacting boson-fermion model Vervier et al. [53], Čule and Paar [54] and Van Isacker and Jolie [55] have developed formulae for the description of level schemes of nuclei around ^{76}As .

The new, more complete level schemes of ^{74}As and ^{73}As obtained in our work [11], offered a new possibility of checking the validity of the supersymmetry scheme. According to this scheme the energy spectra of four nuclei (in the present case of ^{74}Se , ^{75}Se , ^{73}As , and ^{74}As) are interrelated and are described by the same Hamiltonian. The main advantage of this symmetry based approximation is that the eigenvalue problem can be solved analytically.

According to Van Isacker and Jolie [55] the eigenvalues of the Hamiltonian, the energies of the excited states are given by the following formula:

$$\begin{aligned}
 E = & A_{\pi\nu} \sum_i N_i(N_i + 7 - 2i) + A_{\pi} \sum_i N_{i\pi}(N_{i\pi} + 7 - 2i) + \\
 & + A_{\nu} \sum_i N_{i\nu}(N_{i\nu} + 7 - 2i) + B_1 \sum_i n_i + \\
 & + B_2 \sum_i n_i(n_i + 6 - 2i) + C [v_1(v_1 + 3) + v_2(v_2 + 1)] + \\
 & + DL(L + 1) + ES(S + 1) + FJ(J + 1), \quad (11)
 \end{aligned}$$

where N_i , $N_{i\pi}$, $N_{i\nu}$, n_i , v_1 , v_2 , L , S , J are quantum numbers and $A_{\pi\nu}$, A_{π} , A_{ν} , B_1 , B_2 , C , D , E , F are parameters, which are not determined by the symmetry. Formula (11) was obtained for the $U(5)$ limit of the $U_{\pi}(6/12) \otimes U_{\nu}(6/12)$ supersymmetry (SUSY) (proton particle, neutron hole case and $[N_i] \neq [N + 1, 1^5]$). (Somewhat different formula has been derived for $[N_i] = [N + 1, 1^5]$, but only few levels belong to this group representations below 600 keV).

First we fitted the parameters of formula (11) to the levels of the even-even ^{74}Se , odd- A ^{75}Se , and ^{73}As nuclei by a least squares method. Quantum numbers were assigned to the states of the supermultiplet on the basis of energies, spins, parities, decay properties, available one-nucleon transfer reaction spectroscopic factors, as well as IBF(F)M and SUSY wave functions of the levels considered. The obtained parameters were as follows: $A_{\pi} + A_{\pi\nu} = 55$, $A_{\nu} + A_{\pi\nu} = 26$, $B_1 = 525$, $B_2 = 0$, $C = 4$, $D = -28$, a high negative value for E , and $F = 41$ (all in

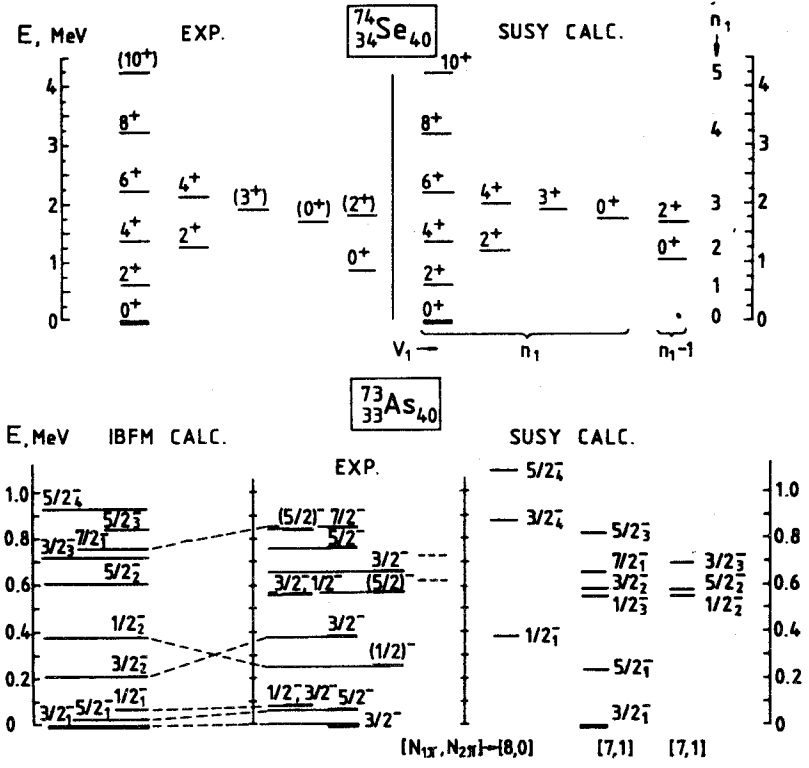


Fig.18. Upper part: Experimental energy levels of ^{74}Se [56] in comparison with the SUSY calculations. Lower part: Experimental energy levels of ^{73}As [40,10] in comparison with the IBFM and SUSY calculations

keV). Then we used these parameters to generate the level spectrum of ^{74}As . (The $A_{\pi\nu}$ was taken-zero, after testing its role in the generated ^{74}As spectrum.)

The experimental and calculated energy spectra are compared in Figs.18 and 19.

The supersymmetry calculations describe 44 levels of four different nuclei reasonably well with 7 fitted parameters only. However, problem appears with additional 1^+ and 3^+ states in the low-energy SUSY spectrum, and the assignment of some SUSY states to experimental ones cannot be made unambiguously.

The supersymmetry calculations and results are described in detail in [12].

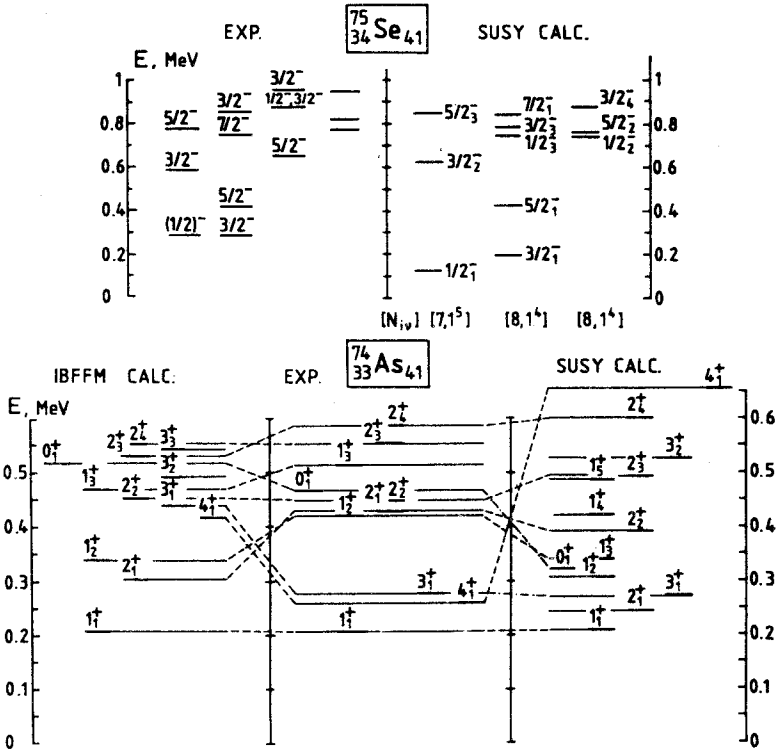


Fig.19. Upper part: Experimental energy levels of ^{75}Se [57] in comparison with the SUSY calculations. Lower part: Experimental energy levels of ^{74}As [11] in comparison with the IBFFM [11] and SUSY [12] calculations. If the assignment of calculated levels to experimental ones is made on the energies only, it is marked with ---

We are indebted to all co-authors of Refs.[4—14] for effective collaboration. The financial support of the Hungarian National Scientific Foundation (OTKA, grant No.3004) is gratefully acknowledged.

REFERENCES

1. Fényes T., Dombrádi Zs., Krasznahorkay A., Gulyás J., Timár J., Kibédi T., Paar V. — *Fizika*, 1990, 22, p. 273.
2. Fényes T., Dombrádi Zs., Gácsi Z., Gulyás J. — *Acta Phys. Hung.*, 1992, 71, p. 239.

3. **Árvay Z., Fényes T., Füle K., Kibédi T., László S., Máté Z., Móri Gy., Novák D., Tárkányi F.** — Nucl. Instr. Meth., 1980, 178, p. 85; **Kibédi T., Gácsi Z., Krasznahorkay A., Nagy S.** — Inst. of Nucl. Res., Debrecen, ATOMKI Ann. Rep., 1986, p. 55; **Kibédi T., Gácsi Z., Krasznahorkay A.** — Inst. of Nucl. Res., Debrecen, ATOMKI Ann. Rep., 1987, p. 100.
4. **Timár J., Quang T.X., Fényes T., Dombrádi Zs., Krasznahorkay A., Kumpulainen J., Julin R., Brant S., Paar V., Šimičić Lj.** — Nucl. Phys., 1994, A537, p. 61.
5. **Timár J., Quang T.X., Fényes T., Dombrádi Zs., Krasznahorkay A., Kumpulainen J., Julin R.** — Nucl. Phys., 1993, A552, p. 149.
6. **Timár J., Quang T.X., Dombrádi Zs., Fényes T., Krasznahorkay A., Brant S., Paar V., Šimičić Lj.** — Nucl. Phys., 1993, A552, p. 170.
7. **Fényes T., Gulyás J., Kibédi T., Krasznahorkay A., Timár J., Brant S., Paar V.** — Nucl. Phys., 1984, A419, p. 557.
8. **Podolyák Zs., Fényes T., Timár J.** — Preprint of Inst. of Nucl. Res. (ATOMKI), Debrecen, 2-1994-P; and Nucl. Phys., 1995, A584, p. 60.
9. **Sohler D., Algora A., Fényes T., Gulyás J., Brant S., Paar V.** — Preprint of Inst. of Nucl. Res. (ATOMKI), Debrecen, 4-1994-P; and to be published.
10. **Sohler D., Podolyák Zs.** — private communication.
11. **Algora A., Sohler D., Fényes T., Gácsi Z., Brant S., Paar V.** — Preprint of Inst. of Nucl. Res. (ATOMKI), Debrecen, 3-1994-P; and Nucl. Phys. A in print.
12. **Algora A., Fényes T., Dombrádi Zs., Jolie J.** — Preprint of Inst. of Nucl. Res. (ATOMKI), Debrecen, 6-1994-P; and Z. Phys. A in print.
13. **Fényes T., Algora A., Podolyák Zs., Sohler D., Timár J., Paar V., Brant S., Šimičić Lj.** — Proc. Int. Conf. on Perspectives for the Interacting Boson Model, Padova, 13—17 June, 1994, eds. R.F.Casten et al., World Sci., Singapore, 1994, p. 673.
14. **Gácsi Z., Gulyás J., Kibédi T., Koltay E., Krasznahorkay A., Fényes T.** — Izv. AN SSSR, ser. fiz., 1983, 47, p. 45.
15. **Fournier R., Kroon J., Hsu T.H., Hird B., Ball G.C.** — Nucl. Phys., 1973, A202, p. 1.
16. **Paar V.** — Nucl. Phys., 1979, A331, p. 16.
17. **Paar V.** — In: In-Beam Nuclear Spectroscopy, vol.2, eds. Dombrádi Zs., Fényes T. (Akad. Kiadó, Budapest, 1984) p. 675; In: Capture Gamma-Ray Spectroscopy, AIP Conf. Proc. 125, Am. Inst. of Phys., N.Y., 1985, p. 70.
18. **Brant S., Paar V., Vretenar D.** — Z. Phys., 1984, A319, p. 351; **Paar V., Sunko D.K., Vretenar D.** — Z. Phys., 1987, A327, p. 291.
19. **Kibédi A., Dombrádi Zs., Fényes T., Krasznahorkay A., Timár J., Gácsi Z., Passoja A., Paar V., Vretenar D.** — Phys. Rev., 1988, C37, p. 2391; **Gácsi Z., Dombrádi Zs., Fényes T., Brant S., Paar V.** — Phys.Rev., 1991, C44, p. 642.
20. **Lopac V., Brant S., Paar V., Schult O.W.B., Seyfarth H., Balantekin A.B.** — Z.Phys., 1986, A323, p. 491.
21. **Arima A., Iachello F.** — Phys. Rev. Lett., 1975, 35, p.157; Ann. of Phys. (N.Y.) 1976, 99, p. 253; 1978, 111, p. 201; 1979, 123, p. 468.

22. **Iachello F., Arima A.** — *The Interacting Boson Model*, Cambridge Univ. Press, Cambridge, 1987.
23. **Iachello F., Scholten O.** — *Phys. Rev. Lett.*, 1979, 43, p. 679.
24. **Scholten O.** — *Prog. in Part. and Nucl. Phys.*, 1985, 14, p. 189; Ph. D. Thesis, Univ. of Groningen (1980).
25. **Bonatsos D.** — *Interacting Boson Models of Nuclear Structure*, Clarendon, Oxford, 1988.
26. **Janssen D., Jolos R.V., Dönauf F.** — *Nucl. Phys.*, 1974, A224, p. 93.
27. **Paar V., Brant S., Canto L.F., Leander G., Vouk M.** — *Nucl. Phys.*, 1982, A378, p. 41.
28. **Paar V.** — In: *Interacting Bosons in Nuclear Physics*, ed. Iachello F., Plenum Press, New York, 1979, p. 163.
29. **Brant S., Paar V., Vretenar D.** — *Computer Code IBFFM/OTQM IKP Jülich*, 1985, unpublished.
30. **Passoja A., Julin R., Kantele J., Kumpulainen J., Luontama M., Trzaska W.** — *Nucl. Phys.*, 1985, A438, p. 413; **Halbert M.L.** — *Nucl. Data Sheets*, 1979, 28, p. 179.
31. **Ward N.J., Tuli J.K.** — *Nucl. Data Sheets*, 1986, 47, p. 135; **Nilson K., Spanier L., Erlandsson B., Vierinen K., Eskola K., Savolainen S.** — *Nucl. Phys.*, 1987, A475, p. 207.
32. **Mo J. N., Sen S.** — *Nucl. Data Sheets*, 1983, 39, p. 741.
33. **Daehnick W.W., Shastry S., Spisak M.J., Gur D.** — *Phys. Rev.*, 1977, C15, p. 1264.
34. **Bhat M.R.** — *Nucl. Data Sheets*, 1988, 55, p. 1.
35. **Bhat M.R.** — *Nucl. Data Sheets*, 1989, 58, p. 1.
36. **Bhat M.R.** — *Nucl. Data Sheets*, 1993, 68, p. 117.
37. **Bhat M.R.** — *Nucl. Data Sheets*, 1993, 68, p. 579.
38. **Mariscotti M.A.J., Behar M., Filevich A., García Bermúdez G., Hernández A.M., Kohan C.** — *Nucl. Phys.*, 1976, A260, p. 109.
39. **King M.M.** — *Nucl. Data Sheets*, 1989, 56, p. 1.
40. **King M.M., Chou W.-T.** — *Nucl. Data Sheets*, 1993, 69, p. 857.
41. **García Bermúdez G., Behar M., Filevich A., Mariscotti M.A.J.** — *Phys. Rev.*, 1976, C14, p. 1776.
42. **Fournier R., Hsu T.H., Kroon J., Hird B., Ball G.C.** — *Nucl. Phys.*, 1972, A188, p. 632.
43. **Rosner B., Mordechai S., Pullen D.J.** — *Nucl. Phys.*, 1973, A206, p. 76.
44. **Hübner A.** — *Z. Phys.*, 1965, 183, p. 25.
45. **Bertschat H., Kluge H., Leithäuser U., Recknagel E., Spellmeyer B.** — *Nucl. Phys.*, 1975, A249, p. 93.
46. **Hogervorst W., Helms H.A., Zaal G.J., Bouma J., Block J.** — *Z. Phys.*, 1980, A294, p. 1.
47. **Döring J., Tabor S.L., Holcomb J.W., Johnson T.D., Riley M.A., Womble P.C.** — *Phys. Rev.*, 1994, C49, p. 2419.
48. **Paar V.** — *Nucl. Phys.*, 1973, A211, p. 29.

49. **Raghavan P.** — *At. Data and Nucl. Data Tables*, 1989, 42, p. 189.
50. **Bădică T., Cojocaru V., Pantelică D., Popescu I., Scîntei N.** — *Nucl. Phys.*, 1991, A535, p. 425.
51. **Ten Brink B.O., Akkermans J., Van Nes P., Verheul H.** — *Nucl. Phys.*, 1979, A330, p. 409.
52. **Kimura K., Takagi N., Tanaka M.** — *Nucl. Phys.*, 1976, A272, p. 381.
53. **Vervier J., Van Isacker P., Jolie J., Kota V.K.B., Bijker R.** — *Phys. Rev.*, 1985, C32, p. 1406.
54. **Čule D., Paar V.** — *Fizika*, 1988, 20, p. 99.
55. **Van Isacker P., Jolie J.** — *Nucl. Phys.*, 1989, A503, p. 429.
56. **Singh B., Viggars D.A.** — *Nucl. Data Sheets*, 1987, 51, p. 225.
57. **Singh B.** — *Nucl. Data Sheets*, 1990, 60, p. 735.
58. **Pfeiffer L., Kovács T., Celler G.K., Gibson J.M., Lines M.E.** — *Phys. Rev.*, 1983, B27, p. 4018.
59. **Arima A.** — *J. Phys. Soc. Japan, Suppl.*, 1973, 34, p. 205.
60. **Towner I.S., Khanna F.C., Häusser O.** — *Nucl. Phys.*, 1977, A277, p. 285.
61. **Mayerhofer U., von Egidy T., Jolie J., Börner H.G., Colvin G., Judge S., Krusche B., Robinson S.J., Schreckenbach K., Brant S., Paar V.** — *Z. Phys.*, 1991, A341, p. 1.